172908-JCI-RG-RV-2 (*Revised*)

Kisspeptin signaling in astrocytes modulates the reproductive axis

Encarnacion Torres[1,2,3], Giuliana Pellegrino[4,†], Melissa Granados-Rodríguez[1,2,3,†], Antonio C. Fuentes-Fayos[1,2,3], Inmaculada Velasco[1,2,3], Adrian Coutteau-Robles[4], Amandine Legrand[4], Marya Shanabrough[5], Cecilia Perdices-Lopez[1,2,3], Silvia Leon[1,2,3], Shel H. Yeo[6], Stephen M. Manchishi[6], Maria J. Sánchez-Tapia[1,2,3], Victor M. Navarro[9], Rafael Pineda[1,2,3], Juan Roa[1,2,3], Fred Naftolin[7], Jesus Argente[8,10,11], Raul M. Luque[1,2,3,8], Julie A. Chowen[8,10], Tamas L. Horvath[5], Vincent Prevot[4], Ariane Sharif[4], William H. Colledge[6], Manuel Tena-Sempere*[,1,2,3,8], Antonio Romero-Ruiz*[,1,2,3]

[†] *Equally contributed and should be considered joint second authors*

***** *Equal senior and corresponding authors*

[1]Instituto Maimónides de Investigación Biomédica de Córdoba (IMIBIC), Córdoba, Spain; [2]Department of Cell Biology, Physiology and Immunology, University of Córdoba, Córdoba, Spain; [3]Hospital Universitario Reina Sofía, Córdoba, Spain; [4]University of Lille, Inserm, CHU Lille, Laboratory of Development and Plasticity of the Neuroendocrine Brain, Lille Neurosciences & Cognition, UMR-S1172, Lille, France; [5]Program in Integrative Cell Signaling and Neurobiology of Metabolism, Department of Comparative Medicine, Yale University School of Medicine, New Haven, USA; [6]Reproductive Physiology Group, Physiology, Development and Neuroscience, University of Cambridge, Cambridge, UK; [7]Centro Fecundacion In Vitro Angela Palumbo, La Laguna, Spain; [8]CIBER Fisiopatología de la Obesidad y Nutrición, Instituto de Salud Carlos III, Madrid, Spain; [9]Division of Endocrinology, Diabetes, and Hypertension, Brigham and Women's Hospital, Harvard Medical School, Boston, USA; [10]Department of Endocrinology, Hospital Infantil Universitario Niño Jesús, Instituto de Investigación La Princesa, and IMDEA-Food Institute, CEI-UAM+CSIC Madrid, Spain; [11]Department of Pediatrics, Universidad Autónoma de Madrid, Madrid, Spain.

Short Title: Kisspeptin signaling in astrocytes

Key Words: Astrocytes, GFAP, kisspeptin receptor (Kiss1r), kisspeptin, GnRH, gonadotropins, metabolic stress, reproduction, neuroendocrinology

**** Corresponding authors:*** **Manuel Tena-Sempere** (fi1tesem@uco.es; Phone:+34957213746);
Antonio Romero-Ruiz (b72rorua@uco.es; Phone:+34957218082)
Department of Cell Biology, Physiology & Immunology
Faculty of Medicine, University of Córdoba
Avda. Menéndez Pidal s/n. 14004 Córdoba, SPAIN

Abstract

Reproduction is safeguarded by multiple, often cooperative regulatory networks. Kisspeptin signaling, via KISS1R, plays a fundamental role in reproductive control, primarily by regulation of hypothalamic GnRH neurons. We disclose herein a pathway for direct kisspeptin actions in astrocytes that contributes to central reproductive modulation. Protein-protein-interaction and ontology analyses of hypothalamic proteomic profiles after kisspeptin stimulation revealed that glial/astrocyte markers are regulated by kisspeptin in mice. This glial-kisspeptin pathway was validated by the demonstrated expression of *Kiss1r* in mouse astrocytes in vivo and astrocyte cultures from humans, rats and mice, where kisspeptin activated canonical intracellular signaling-pathways. Cellular co-expression of *Kiss1r* with the astrocyte markers, GFAP and S100β, occurred in different brain regions, with higher percentage in Kiss1- and GnRH-enriched areas. Conditional ablation of *Kiss1r* in GFAP-positive cells, in the G-KiRKO mouse, altered gene expression of key factors in PGE_2 synthesis in astrocytes, and perturbed astrocyte-GnRH neuronal appositions, as well as LH responses to kisspeptin and LH pulsatility, as surrogate marker of GnRH secretion. G-KiRKO mice also displayed changes in reproductive responses to metabolic stress induced by high-fat diet, affecting female pubertal onset, estrous cyclicity and LH-secretory profiles. Our data unveil a non-neuronal pathway for kisspeptin actions in astrocytes, which cooperates in fine-tuning the reproductive axis and its responses to metabolic stress.

Significance statement

We characterize herein a brain non-neuronal pathway for direct kisspeptin actions in astrocytes, that contributes to fine tune reproductive function and its modulation by metabolic status.

Introduction

Reproduction, indispensable for continuation of species, is regulated by sophisticated mechanisms, which integrate central and peripheral inputs, acting at different levels of the hypothalamic-pituitary-gonadal (HPG) axis. Reproductive capacity absolutely relies on the pulsatile secretion of gonadotropin-releasing hormone (GnRH), the hypothalamic neuropeptide that drives the secretory pulses of pituitary gonadotropins, luteinizing hormone (LH) and follicle-stimulating hormone (FSH), which in turn govern gonadal function (1). GnRH neurosecretion takes place in two main patterns: the surge and pulse modes (2). The surge mode occurs exclusively in females and is key for the induction of the preovulatory peak of LH that triggers ovulation. The pulse mode is negatively regulated by sex steroids in both sexes, and dictates proper gonadotropin secretory profiles to drive gametogenesis and steroidogenesis.

The central position of GnRH neurons in reproductive control makes them the target of different regulatory pathways. Among these, kisspeptins, encoded by the *Kiss1* gene and acting via the G-protein coupled receptor, KISS1R (aka GPR54), have been recognized as key elicitors of GnRH secretion and essential players in the central regulation of puberty, gonadotropin secretion and fertility (3). Kisspeptins act primarily on GnRH neurons, which express *Kiss1r* and are potently activated by kisspeptins (1, 3). Functional genomic studies documented that kisspeptin actions on GnRH neurons suffice for attainment of reproductive capacity (4), while elimination of *Kiss1r* selectively from GnRH cells caused central hypogonadism (4, 5). However, *Kiss1r* expression has been found in multiple brain areas not harboring GnRH neurons and central kisspeptin actions at targets other than GnRH neurons are needed for modulation of the reproductive axis (6). However, the nature and physiological relevance of such non-GnRH targets of kisspeptins are ill defined, and the down-stream effectors of kisspeptin actions remain largely unknown. No evidence for non-neuronal targets of kisspeptins at central levels has been presented to date.

Two main populations of Kiss1 neurons have been found in the hypothalamus, one in the arcuate nucleus (ARC) and the other in the rostral hypothalamic area, mainly the anteroventral peri-ventricular nucleus (AVPV) in rodents (3). ARC Kiss1 neurons, which are found in both sexes, mediate the negative feedback effect of sex steroids and are a key component of the GnRH pulse generator (7). In contrast, AVPV Kiss1 neurons display a clear sex dimorphism, with predominant presence in females, and are involved in mediating the positive feedback effect of estradiol and the generation of the preovulatory GnRH/LH surge (8). Projections of Kiss1 neurons to multiple hypothalamic and extra-hypothalamic areas have been documented (9), while non-synaptic contacts of Kiss1 neurons with GnRH neurons have been recently documented, suggesting volume transmission (10).

GnRH neurosecretion is also modulated by glial cells, of which astrocytes are the most abundant subtype. Astrocytes are known to play a critical role in the regulation of reproductive function; the bi-directional interaction between astrocytes and GnRH neurons, and their adhesiveness, being essential for proper reproductive control (11-13). Astrocytes are abundantly located in the vicinity of GnRH neurons (14) and ensheath them, with several adhesion factors being expressed in both astrocytes and GnRH neurons to permit homophilic interactions (12). Plastic changes in astrocyte morphology and their contacts with GnRH neurons have been demonstrated in different states of the reproductive axis (15). Moreover, astrocytes respond to key reproductive regulators, such as gonadal steroids (16), and produce different signals, including growth factors (e.g., IGF-1, TFGβ and EGF family members), neurotransmitters (e.g., glutamate) and prostaglandins (e.g., PGE_2) (11, 12, 17), that modulate GnRH neurosecretory activity. Astrocytes are also sensitive to metabolic cues, e.g., leptin, ghrelin (18, 19), known to influence reproductive function, and insulin was recently shown to act in astrocytes to funnel at least part of its modulatory actions on puberty onset and gonadal function in mice (20).

In the context of our search for novel brain targets of kisspeptins, we report herein the characterization of a pathway involving kisspeptin signaling in astrocytes, a non-neuronal target in the brain, initially identified by proteomic analyses and defined further by expression and functional genomic studies.

Results

Proteomic identification of novel kisspeptin targets in the hypothalamus

We used *Kiss1*-null mice to identify hypothalamic targets modulated by kisspeptins, by applying quantitative proteomics following a bolus of kisspeptin-10 (Kp-10). Since Kiss1 KO mice are devoid of endogenous levels of kisspeptin (21), we hypothesized this would increase the capacity to detect changes in expression of kisspeptin-responsive proteins after stimulation with an effective but sub-maximal dose of Kp-10 (50 pmol), selected to avoid supra-physiological stimulation. To exclude detection of rapid post-translational changes (e.g., in intracellular signaling cascades), hypothalamic tissue was obtained 60-min after icv injection of Kp-10, a time-point when a significant elevation of serum LH levels was detected (4.41 ± 0.25 ng/mL vs. 1.0 ± 0.30 ng/mL in vehicle-treated animals; P=0.0012), confirming the efficacy of the dose and time selected to activate the gonadotropic axis (22).

Nano-HPLC/mass spectrometry (MS), equipped with SWATH acquisition for label-free quantitative proteomics, identified a set of differentially-expressed proteins in the hypothalamic preoptic area (POA), following icv injection of Kp-10 (**Figure 1A**). These proteins were categorized/displayed in Protein-Protein Interaction (PPI) networks, biological processes defined by gene ontology (GO), and enrichment analyses based on cellular component GO terms (TOP10). The STRING database identified PPI networks of 77 differentially-expressed proteins, with three main clusters being found. CLUSTER-1 included components of the mitochondrial respiratory chain. The most robust association, CLUSTER-2, was centered around ribosomal proteins (RPs), while an independent network, CLUSTER-3, was organized around glial fibrillary acidic protein, GFAP, major component of cytoskeleton and putative marker of astrocytes (23) (**Figure 1B**).

GO-enrichment analyses identified different biological pathways putatively modulated by kisspeptin in the hypothalamic POA, including among others, cytoplasmic translation, structural constituents of the cytoskeleton, oxidative phosphorylation, regulation of oxidative stress-induced neuron death and, notably, astrocyte development (**Figure 1C**). Of the top 10 variables identified by an enrichment analysis using GO terms, astrocyte end-foot and astrocyte projections, identified in CLUSTER-3, were classified as two of the most significant categories based on their adjusted P value and gene ratio, suggesting a potential modulation of astrocyte-molecular processes by kisspeptin (**Figure 1D**).

We further analyzed the raw SWATH-MS data in order to provide individual validation of the changes in GFAP, Amyloid Precursor Protein (APP) and Metallothionein 3 (MT3) levels in the POA after kisspeptin stimulation; APP and MT3 were also visualized in CLUSTER-3 of the PPI network. Our analyses

132 documented that kisspeptin upregulated GFAP levels in the POA, whereas the expression levels of APP
133 and MT3 were significantly decreased following Kp-10 injection to Kiss1 KO mice (**Figure 1E**).

134 In a parallel confirmatory approach, two-dimensional difference gel electrophoresis (2D-DIGE) was
135 applied to an independent set of POA samples from Kiss1 KO mice icv injected with Kp-10. DIGE
136 analyses detected 30 differentially-expressed proteins, identified by MS. Ontology analysis revealed
137 factors involved in cellular metabolism and energy balance, cell signaling, protein folding and synaptic
138 plasticity. Of note, approximately 34% of these differentially expressed proteins were allocated to the
139 category of synaptic plasticity, and included GFAP as an altered protein in response to kisspeptin (**Figure**
140 **1F**). These DIGE results confirmed our data from SWATH-based quantitative proteomics, suggesting
141 kisspeptin regulation of key astrocyte markers.

142 *Characterization of a kisspeptin pathway in astrocytes*

143 To confirm the putative regulatory actions of kisspeptin in astrocytes, the expression of GFAP and
144 vimentin, which is also produced in developing and activated astrocytes, was independently evaluated,
145 at the mRNA and protein levels, in the POA of Kiss1 KO mice following icv injection of Kp-10. These
146 analyses confirmed the proteomic data since expression of both putative astrocyte markers was increased
147 in POA after central kisspeptin stimulation (**Figure 2A**). *Kiss1r* mRNA expression was assessed also in
148 primary astrocyte cultures from wild-type neonatal rats and mice, as well as humans. Expression of *Kiss1r*
149 was demonstrated in astrocytes of both rodent species and humans, with comparable Ct values in real-
150 time PCR analyses between humans and mice. In contrast, *Kiss1* expression was not detected in
151 astrocyte cultures, from rats or mice (**Figure 2B**).

152 Using primary cultures from neonatal rodents, we interrogated whether key elements of the canonical
153 intracellular signaling pathways are activated by kisspeptin in astrocytes. Kp-10 treatment induced the
154 phosphorylation of ERK/MAP kinase, a pivotal component of the kisspeptin signaling pathway in target
155 cells (24), in rat hypothalamic astrocytes, with peak levels at 10-min after stimulation (**Figure 2C**). In
156 addition, an increase in the level of phosphorylation of AKT was observed at 10-min after kisspeptin
157 stimulation. Kp-10 treatment stimulated also the phosphorylation of ERK/MAP kinase in primary cultures
158 of mouse hypothalamic astrocytes, but not in cortical astrocytes. In mice, however, Kp-10 did not
159 stimulate the phosphorylation of AKT in either hypothalamic or cortical astrocytes (**Figure 2D**).

160 We assessed also whether astrocyte markers, GFAP and S100β, are co-expressed with *Kiss1r* in vivo
161 in various brain areas of control female mice at diestrus. Double labelling analyses, using RNAscope in
162 situ hybridization to detect *Kiss1r* and *GnRH* mRNA, and immunohistochemistry to detect GFAP- and

S100β-positive cells, conclusively showed not only that GnRH neurons co-express *Kiss1r*, in line with previous reports (25), but also that *Kiss1r* expression is detectable in GFAP/S100β-expressing cells in different hypothalamic areas involved in the control of the reproductive axis, as the *organum vasculosum lamina terminalis* (OVLT), AVPV and ARC, as well as the cortex, used as non-neuroendocrine reference control. For representative examples of individual labelling, and *Kiss1r*/GFAP/S100β or *Kiss1r*/*GnRH* positive cells in the OVLT, see **Figure 3A-H**. Quantitative analyses documented an enrichment in the % of co-localization of *Kiss1r* and GFAP/S100β in OVLT (73%) and AVPV (67%), areas in which GnRH and Kiss1 neuronal populations are found, as well as in the ARC (72%), where terminals of GnRH neurons project into the median eminence and other prominent Kiss1 neuronal population is found. In the cortex, although there was detectable co-localization between *Kiss1r* and GFAP/S100β, the percentage of double positive cells was lower than in the former brain areas (**Figure 3I**).

In addition, we explored the existence of intimate appositions between astrocytes and Kiss1 neurons, as anatomical substrate for kisspeptin actions on *Kiss1r*-expressing astrocytes in vivo. We applied immunohistochemical detection of GFAP and kisspeptin in control female mice, with particular focus on the AVPV and ARC. Confocal images and 3D reconstructions documented clear close appositions between astrocyte processes (denoted by GFAP-immunoreactivity) and Kiss1 neurons, at the level of cell bodies and fibers, in the AVPV and ARC, respectively (**Figure 3J-K**). These contacts were consistently observed across the different AVPV and ARC sections and individuals studied. We also evaluated changes in the number of contacts between kisspeptin fibers and GnRH neurons across the ovarian cycle, and the potential interaction with astrocyte processes. While in metestrus and diestrus, ~40% of GnRH neurons were contacted by kisspeptin fibers, the number of appositions drop dramatically to <10% in the morning (10:00 am) of proestrus, i.e., before the initiation of the pre-ovulatory surge, but raised thereafter through the early afternoon of proestrus (55%) until the morning of estrus, reaching values >70% of GnRH neurons receiving kisspeptin contacts (**Figure 3L**). Notably, kisspeptin fibers, when in contact with GnRH neurons, were in close proximity to GFAP-labelled processes (**Figure 3M**).

Astrocytic expression of *Kiss1r* in vivo was documented also by qPCR analyses of astrocytes isolated from control male and female mice using fluorescence-activated cell sorting (FACS). Sorting procedures were optimized and validated by expression analyses in the mediobasal hypothalamus (MBH) of female mice, which documented substantial enrichment of astrocyte abundantly-expressed genes, such as *Gfap*, *Glast* and *Cx43*, in the astrocyte-positive fraction, whereas neuronal- (*Elavl3/Huc*, *RBFox3/NeuN*), microglial- (*Aif1/Iba1*) and endothelial- (*CD31*) expressed genes were enriched in the negative fraction

(**Figure 4A-B**). Expression analyses of *Kiss1r* in astrocytes obtained from the POA, MBH and cortex of male and female mice revealed unambiguous expression in the astrocyte-positive fraction in all areas analyzed, with grossly similar profiles in both sexes (**Figure 4C**). In fact, of the 36 positive fractions (3 regions x2 sexes x6 animals per group) tested**,** *Kiss1r* expression was detectable in 33, with a mean Ct value=21.9. Aggregated expression analysis per region documented higher levels in the FACS-negative vs. positive fraction only in the POA, in line with the abundant expression of *Kiss1r* in GnRH neurons (3), with *Kiss1r* expression being detectable in the three areas analyzed (**Figure 4D**).

Analysis of kisspeptin signaling in astrocytes in vivo: Studies in the G-KiRKO mouse

To interrogate the physiological relevance of direct kisspeptin actions in astrocytes, we generated a mouse line with conditional ablation of *Kiss1r* in GFAP-expressing cells, *by* crossing a well-validated Gfap-Cre mouse line (26) with a *Kiss1r* $^{lox/lox}$ mouse line, previously used in our group for kisspeptin receptor ablation in vivo (27, 28). This mouse line was named G-KiRKO, for *GFAP-specific Kiss1 Receptor KO* (**Supplemental Fig S1A**). To validate this line, PCR was applied for detecting the recombination event at the loxP sites of *Kiss1r* gene, denoting effective Cre activity and gene inactivation. Effective recombination took place in the brain of G-KiRKO mice, abundantly in the POA and, to a lesser extent, in the MBH (**Supplemental Figure S1B**). Very low to negligible recombination was detected in the lung or white and brown adipose tissues, as reference peripheral tissue controls, while recombination was also found in the testis, where Gfap expression has been documented in Leydig cells (29).

In line with effective hypothalamic recombination, *Kiss1r* mRNA levels in astrocyte cultures from G-KiRKO mice were low to negligible, in contrast to control astrocytes and hypothalamic tissue from control mice (**Supplemental Figure S1B**). Functional studies in primary cultures of astrocytes from the hypothalamus of control and G-KiRKO mice evidenced a significant increase (>35%) in phospho-ERK levels, 10-min after Kp-10 treatment in astrocytes of control mice, while no significant changes in ERK phosphorylation were observed in astrocytes from G-KiRKO mice after kisspeptin challenge. Detectable expression of GFAP, but not the neuronal marker, NeuN, was found in our astrocyte primary cultures, denoting glial lineage and absence of neuronal contamination. No significant change in GFAP protein content was found in cultures from control or G-KiRKO mice after short-term (10-min) challenge with Kp-10 (**Supplemental Figure S1C**), seemingly due to the small window of stimulation.

Further evidence for targeted Cre activity in astrocytes in vivo was obtained using a reporter mouse line, generated by crossing the Gfap-Cre mouse with a reporter line in which YFP (yellow fluorescent protein) is expressed upon Cre-mediated recombination. Using GFAP and S100β as astrocyte makers to

detect not only processes but also the cytosolic shape of astrocytes, we found that about 92%, 89% and 95% of GFAP/S100β-positive cells co-expressed YFP (denoted by GFP-immunostaining) in the ARC, AVPV and OVLT areas, respectively (**Supplemental Figure S2A,C**). This strong astrocyte-predominant effective recombination was also supported by the fact only 25-30% of non-astrocytic, NeuN positive cells in the above areas displayed GFP-immunoreactivity (**Supplemental Figure S2B,D**).

G-KiRKO mice were assessed for somatic and pubertal maturation, both under normal (chow) diet and after metabolic challenge with 58% HFD from weaning. No differences in body weight (BW) gain were detected between genotypes, irrespective of the feeding regimen, either in females (**Supplemental Figure S3A-B**) or males (**Supplemental Figure S4A-B**). G-KiRKO female mice under chow diet displayed conserved ages of puberty onset, denoted by vaginal opening (VO; **Figure 5A**), and first estrus (FE; **Supplemental Figure S3C**). In contrast, while control females fed a HFD showed a marked advancement of the mean age of VO, this effect was blunted in G-KiRKO female mice under HFD, whose mean age of VO was similar to that of control mice fed chow diet (**Figure 5B**). Yet, no clear differences were detected in the age of FE between control and G-KiRKO mice fed a HFD (**Supplemental Figure S3D**). In adulthood, icv stimulation with a submaximal dose of Kp-10 (50 pmol) evoked significant LH secretory responses in female control and G-KiRKO mice on chow diet, in line with previous references (22). Yet, the magnitude of Kp-induced LH secretion was significantly higher at peak levels, 15-min after Kp-10 injection, in G-KiRKO females (**Figure 5C**). Female G-KiRKO mice on HFD also displayed higher LH secretory responses to Kp-10 simulation (**Figure 5D**). In addition, HFD exposure induced estrous cycle irregularities in female G-KiRKO mice, with longer cycle length and a higher number of days in diestrus and reduced number of days in estrus. These alterations were not detectable in lean female G-KiRKO mice, as they did not present overt perturbations in individual phases of ovarian cyclicity (**Figure 5E-F**), except for a moderate shortening in the total length of the cycle. Despite the lack of major cycle irregularities, LH secretory patterns in female G-KiRKO mice displayed notable alterations, with a significant lowering of basal LH levels and a trend towards a higher number of LH secretory pulses (peaks) in G-KiRKO animals fed chow diet. Due to variability within the control group, total LH secretion and LH secretory mass per pulse were not significantly decreased, despite a strong trend for decline in total LH secretion (**Figure 5G**). No change in the magnitude of estrogen-primed LH surges, nor overt alterations in fecundity indices, were detected between control and G-KiRKO female mice (**Supplemental Figure S3E-F**). HFD feeding to female G-KiRKO mice worsened LH secretory profiles, as denoted by significantly lower basal LH levels and LH secretory mass per pulse, as well as a strong

trend to decline in total LH secretion (**Figure 5H**). For representative individual LH secretory profiles of female G-KiRKO mice, fed chow or HFD, see **Supplemental Figure S5A-B**.

Reproductive phenotypic markers were less affected in G-KiRKO males, which did not show changes in the age of puberty onset, denoted by balano-preputial separation (BPS), either under chow diet or HFD (**Supplemental Figure S4C-D**). In adulthood, adult male control and G-KiRKO mice showed robust LH responses to 50 pmol icv Kp-10 stimulation, which were significantly higher at 15-min in G-KiRKO vs. controls. Yet, in contrast to females, G-KiRKO males on HFD had LH responses to Kp-10 similar to those of control mice under HFD (**Supplemental Figure S4E**).

The potential impact of congenital deletion of *Kiss1r* in astrocytes on key metabolic parameters was also monitored in adult animals of both sexes. No differences in terms of either BW or body fat and lean mass were detected between genotypes, in either sex or feeding regime (chow vs. HFD; **Supplemental Figure S6A-B**). Regarding glucose homeostasis, basal glucose levels were similar in control and G-KiRKO mice of both sexes. However, glucose-tolerance tests (GTT) revealed a subtle improvement of the response to a glucose bolus in G-KiRKO mice, as denoted by time-course profiles and integral AUC glucose values, over the 120-min period, which were significantly lower in G-KiRKO male mice on chow diet. A similar trend was observed in females, but the reduction in AUC for glucose during the GTT was slightly below the level of statistical significance (**Supplemental Figure S7A-B**). In addition, a moderate improvement of glucose tolerance was also noted in G-KiRKO males fed HFD, which was not detected in null HFD females. G-KiRKO mice of both sexes did not display consistent alterations in insulin sensitivity, measured by insulin-tolerance tests (ITT), under normal or HFD conditions (**Supplemental Figure S7C-D**).

The consequences of specific ablation of *Kiss1r* in astrocytes in terms of their interplay with GnRH neurons were also evaluated. Peripheral administration of an effective dose of Kp-54 was applied, as previously reported (30), and both cFos activation in GnRH neurons and changes in appositions between GFAP-positive and GnRH cells were analyzed. Potent LH responses were found in control and G-KiRKO female mice at 60-min after Kp-54 injection (**Supplemental Fig S8**). No significant differences were detected in the percentage of GnRH neurons expressing cFos between genotypes, albeit considerable variability was observed (**Supplemental Fig S8A**,**D**). However, the number of close appositions between GFAP-positive cells and GnRH neurons was increased in G-KiRKO mice, with this difference reaching statistical significance for interactions at the level of the soma (**Supplemental Fig S8B**,**E-F**), denoting

286 that elimination of kisspeptin signaling in astrocytes may perturb their physical interplay with GnRH
287 neurons.

288 Finally, qPCR analyses were applied to primary cultures of astrocytes from control and G-KiRKO mice
289 to assess the expression levels of a set of genes involved in key aspects of astrocyte physiology. These
290 included molecular factors involved in astrocyte differentiation and proliferation (31-34), elements of the
291 steroidogenic pathway (35), adhesion molecules involved in glia-to-GnRH neuron interactions (36), and
292 factors involved in prostaglandin (PG) synthesis (37). No gene expression changes were detected for
293 differentiation, proliferation, steroidogenic or adhesion factors. In contrast, mRNA levels of some
294 components of the PG synthesis pathway were altered in astrocytes from G-KiRKO mice. Thus, the
295 expression levels of cyclooxygenase genes, *Cox-1* and *Cox-2*, were oppositely changed, with decreased
296 *Cox-1* expression and increased *Cox-2* mRNA levels in G-KiRKO astrocytes. In addition, expression of
297 the gene encoding the inducible microsomal prostaglandin E synthase-1 (*mPges*) was significantly
298 increased in astrocytes lacking *Kiss1r*. Gene expression of other constitutive factors of the PG synthetic
299 pathway, as *Pges-2* and *cPges*, was not altered in astrocyte cultures from G-KiRKO mice (**Figure 6**).

Discussion

Characterization of the entire set of cellular and molecular pathways underlying kisspeptin actions in the hypothalamus remains incomplete. In our search for protein targets of kisspeptins in the preoptic area, i.e., where most GnRH neurons are located (1), we applied label-free quantitative proteomics to identify individual factors, as well as cellular and molecular pathways, modulated by kisspeptin. To maximize our discrimination capacity, we used Kiss1 KO mice, devoid of endogenous kisspeptins, as optimal for detection of protein targets up- or down-regulated after challenge with exogenous kisspeptin. Admittedly, congenital Kiss1 null mice display hypogonadotropic hypogonadism, that might cause some developmental defects due to lower sex steroid levels but, importantly for the purposes of our study, retain proper migration of GnRH neurons into the hypothalamus and kisspeptin responsiveness (21).

PPI analyses on SWATH data allowed identification of proteomic responses to kisspeptin stimulation, as defined by different protein clusters, including elements of the respiratory chain, as well as ribosomal proteins and other factors involved in protein translation, possibly reflecting activation of basic cellular processes needed for kisspeptin effects. Furthermore, our complementary 2D-DIGE proteomic approach revealed different categories regulated by kisspeptin, including proteins involved in cell metabolism, cell signaling and protein folding, in line with the variety of intracellular cascades mediating kisspeptin actions. These kisspeptin-sensitive pathways warrants independent investigation. It must be stressed, however, that our proteomic approach was not intendedly directed to identification of conventional intracellular signaling mediators, e.g., we did not search for rapid phosphoproteomic changes, but aimed to pinpoint major down-stream elements of kisspeptin actions, amenable for confirmation by physiological studies, assuming that the genetic model and time-window of analysis could hamper identification of the whole repertoire of kisspeptin targets.

In this scenario, we were especially attracted by our findings on the putative regulation of astrocytic-related markers by kisspeptin. Indeed, PPI analyses revealed an independent cluster modulated by kisspeptin, centered around GFAP, in which other proteins, such as MT3 and APP, were also identified. MT3 is a zinc-biding metallothionein that contributes to actin polymerization in astrocytes (38), while APP is reportedly induced in reactive glial cells (39). Analysis of raw data from SWATH showed that acute kisspeptin stimulation increased GFAP content in the POA, while it decreased MT3 and APP levels. In addition, 2D-DIGE proteomics identified GFAP as one of the differentially expressed proteins related to synaptic plasticity, whose levels were also altered in response to Kp-10. These data collectively point towards an effect of kisspeptin on astroglial cells. This was further documented by the ability of icv Kp-

10 to increase gene/protein expression levels not only of *Gfap*/GFAP, but also vimentin, another astrocyte marker (40), in the POA of mice. To our knowledge, this is the first evidence supporting the capacity of kisspeptins to modulate non-neuronal brain cells, likely astrocytes. Previous data highlighted the participation of glial cells, and particularly astrocytes, in the control of GnRH neurosecretion, mainly via the release of bioactive molecules, such as PGE_2, and other mechanisms, including juxtacrine interactions with GnRH neurons (13, 41). Yet, no evidence had been presented on a role of astroglial cells as transducers of kisspeptin effects on GnRH neurons, or any other brain target/function.

Admittedly, our proteomic data did not conclusively prove direct kisspeptin actions in astrocytes. Compelling evidence for such putative kisspeptin pathway was provided by a combination of expression and functional studies in control rats and mice. Expression of *Kiss1r*, but not of *Kiss1,* was demonstrated in primary cultures of astrocytes from both rodent species. Notably, similar *KISS1R* expression was also detected in human astrocytes, suggesting the potential conservation of this pathway. Phosphorylation of ERK1/2, canonical element of the kisspeptin signaling pathway, was consistently induced by kisspeptin in rat and mouse astrocytes in culture; increased phosphorylation of AKT was observed also in rat astrocyte cultures at 10-min after kisspeptin stimulation. While it can be argued that astrocyte cultures from neonatal rodents might not fully recapitulate all features of later developmental periods, these have proven valid to evaluate key aspects of astrocyte physiology (42). Additionally, co-localization of *Kiss1r* expression with GFAP and S100β, as canonical markers for detection of astrocyte processes and cell bodies, was conclusively documented in adult mice in vivo, in key brain areas for reproductive control, as the OVLT, with a large proportion of GnRH neurons, AVPV and ARC. Enrichment of *Kiss1r*/GFAP/S100β co-localization was observed in these GnRH-/Kiss1-abundant areas, as compared with the cortex, suggesting that kisspeptin signaling in astrocytes might display some degree of region specificity; a contention further supported by the fact that responses to Kp-10 in terms of ERK1/2 phosphorylation were not detectable in cortical astrocyte cultures. Expression of *Kiss1r* gene in astrocytes from adult male and female mouse brains further supported a tenable kisspeptin signaling pathway in these glial cells under physiological conditions. This contention is reinforced by the close appositions between astrocytic (GFAP-positive) projections and Kiss1 neurons found in key hypothalamic areas, as the ARC and AVPV, providing the potential anatomical substrate for the source of kisspeptin input to astrocytes. Furthermore, the dynamic changes in the number of appositions between kisspeptin fibers and GnRH neurons across the ovarian cycle seemingly engaged also changes in the interplay with GFAP-positive processes, suggesting a role of astrocytes in the modulation of such Kiss1-GnRH neuronal interactions. However,

our anatomical and FACS analyses conclusively documented expression of *Kiss1r* also in brain areas, such as the cortex, not primarily involved in reproductive control, whose role and putative physiological relevance warrant independent investigation.

The physiological role of direct kisspeptin actions in astrocytes was further addressed by functional genomic analyses, assessing reproductive and metabolic markers in our mouse model of congenital ablation of *Kiss1r* in GFAP-expressing cells. While the use of *Gfap*-driven Cre mouse lines might cause targeting of some neuronal lineages, due to potential Cre expression in radial glial cells (43), congenital ablation was posed with obvious advantages in our model, as we intended to explore early maturational events, including puberty, for which inducible models using tamoxifen, are not applicable or have important limitations. Furthermore, constitutive Gfap-Cre mouse lines have been recently used for selective astrocyte activation using optogenetics (44), and to successfully target astrocytes in different models, including constitutional ablation of insulin receptors (20), connexin 43 (45), or interleukin-6 (46) in *Gfap*-expressing cells, in which specific astrocyte targeting was thoroughly documented using reporter mouse lines. In our G-KiRKO model, effective recombination was demonstrated in the vast majority (~90-95%) of astrocytes in relevant hypothalamic areas, including the ARC, AVPV and OVLT, using a genetic reporter model for astrocyte labelling and a combination of two astrocytic markers. In contrast, only 25-30% of non-astrocytic, NeuN-positive cells in these areas showed GFP-immunoreactivity, supporting a clear astrocyte-preferential recombination in our G-KiRKO line. In good agreement, primary astrocyte cultures from conditional null mice displayed low to negligible levels of *Kiss1r* mRNA expression. Collectively, these data confirm the validity of our model.

Effective ablation of *Kiss1r* in GFAP-positive cells failed to impact the timing of puberty in both sexes, that was associated with grossly preserved fertility. However, G-KiRKO mice displayed alterations in the patterns of LH responses to kisspeptin stimulation and LH secretory profiles. These phenotypic features are different from those of global *Kiss1r* KO mice (27), which suffer from severe central hypogonadism, or mice with conditional inactivation of *Kiss1r* in GnRH neurons, which phenocopy global *Kissr1* KO (4, 5), or in POMC neurons, which are devoid of a detectable phenotype (47) (**Supplemental Table S1**). Notably, LH responses to an icv bolus of Kp-10 were not only preserved but even enhanced in mice with *Kiss1r* ablation in astrocytes; a phenomenon that was not observed in global or GnRH-specific *Kiss1r* KO (5, 27), and was more evident in females than in males, suggesting a possible sex difference in the effects of kisspeptin signaling in astrocytes. This finding argues against the possibility of a general recombination affecting neuronal cells driven by our Gfap-Cre model, as this would have resulted in ablation of *Kiss1r* from GnRH neurons and, hence, elimination of LH responses to kisspeptin. Conversely, our data strongly

suggest that kisspeptin signaling in astrocytes might play an acute suppressive role in modulating kisspeptin effects on GnRH neurons. Considering the high potency of the direct effects of kisspeptin on GnRH neurons, such loop would operate as a mechanism for self-restraining the magnitude of GnRH pulses after kisspeptin stimulation. In line with this repressive role, congenital elimination of *Kiss1r* from astrocytes resulted in upregulation of the expression of genes encoding inducible factors involved in PGE_2 synthesis, namely COX-2 and mPGES-1, suggesting that G-KiRKO mice have increased astrocyte production of this PG, which is a major stimulatory signal for GnRH neurons (17). This could explain the enhanced acute LH responses to Kp-10 in mice with ablation of *Kiss1r* in astrocytes. Furthermore, the reduction of *Cox-1* expression in astrocytes from G-KiRKO mice could also contribute to enhanced PGE_2 synthesis, as down-regulation of *Cox-1* has been previously shown to facilitate PGE_2 production in astrocytes (48). These changes did not affect other constitutive elements of the PGE synthesis pathway. Intriguingly, the metabolic hormone, ghrelin, has been shown to induce opposite (stimulatory) responses in terms of PGE_2 synthesis in astrocytes, as a means to modulate other hypothalamic circuits, such as AgRP neurons (19). Since ghrelin may suppress hypothalamic *Kiss1* expression (49), it is plausible that, at least partially, this stimulatory effect could stem from ghrelin's capacity to reduce the inhibitory tone of kisspeptin on the PGE_2 synthetic pathway in astrocytes.

Female G-KiRKO mice displayed differences in the pattern of LH pulsatility, defined by lower basal LH levels and total LH secretion, despite a trend towards a higher number of LH pulses. These secretory alterations were coupled to changes in the number of appositions between astrocytes and GnRH neurons, which were increased in G-KiRKO mice. Recent evidence has documented that ARC Kiss1 neurons are a central component of the GnRH pulse generator (7); our present findings suggest that, in addition to direct effects on GnRH dendrons, kisspeptin actions on astroglial cells may contribute to proper shaping of the secretory profiles of GnRH, denoted by changes in LH pulsatility, as surrogate marker of GnRH. While the trend to an increased number of LH pulses in G-KiRKO mice is compatible with the proposed role of kisspeptin actions in astrocytes, as putative self-restrain mechanism for kisspeptin-induced GnRH secretion, the suppression of basal LH levels and LH secretory mass likely reflects some partial desensitization due to excessive kisspeptin stimulation, which might also be linked to changes in astrocyte-GnRH neurons interactions, as suggestive of perturbations of normal GnRH neuronal ensheathment after ablation of *Kiss1r* in astrocytes. It must be stressed, though, that these changes did not translate into overt alterations of adult reproductive function in basal conditions, except for a modest shortening of the length of the ovarian cycle, suggesting some degree of redundancy of kisspeptin regulatory action on astrocytes, regarding preservation of fertility, as was described previously for *Kiss1* expression itself (50). Of note, despite abundant co-expression of *Kiss1r* and GFAP/S100β in the AVPV,

where Kiss1 neurons involved in pre-ovulatory surge are located, the magnitude of estrogen-primed LH surges was preserved in G-KiRKO female mice. Recent evidence has suggested that positive feedback effects of estradiol also involve stimulation of neuro-progesterone synthesis in hypothalamic astrocytes, which seems to be required for activation of AVPV Kiss1 neuron population, to drive the preovulatory LH surge (51). Our findings in G-KiRKO mice suggest that kisspeptin signaling in astrocytes is dispensable for such positive feedback action of estrogen, and point out a role in the modulation of pulse, but not surge mode of GnRH secretion. In good agreement, no changes in gene expression of key steroidogenic factors were detected in astrocytes from G-KiRKO mice. Likewise, ablation of *Kiss1r* from astrocytes did not perturb markers of proliferation, differentiation or cell adhesion, suggesting that these key functions are not physiologically modulated by direct kisspeptin actions.

Compelling evidence has recently documented that astrocytes play a fundamental role in the brain mechanisms governing energy homeostasis (52, 53), and conditions of metabolic stress, as exposure to HFD, are known to cause reactive changes in astrocytes, which are putatively involved in mediating at least part of the metabolic deregulations associated with obesity (54). Moreover, key hormones, such as leptin and ghrelin, also endowed with important reproductive roles (55), are known to modulate metabolic homeostasis via direct actions in astrocytes (18, 19, 56). In this context, we considered it relevant to evaluate the reproductive phenotype of G-KiRKO mice under an obesogenic diet, which revealed a sex-biased impact. While HFD exposure caused an acceleration of puberty onset in control female mice, in line with previous reports in rats (57), conditional ablation of *Kiss1r* in astrocytes largely prevented this effect, suggesting that astrocytic responses to HFD, putatively involved in advancing pubertal onset in the female, are partially prevented in the absence of kisspeptin signaling in astrocytes. In contrast, no differences in pubertal timing were noted between male control and G-KiRKO mice fed HFD. Of note, the effect observed in pubertal G-KiRKO females was more evident in terms of the vaginal opening, which denotes initiation of puberty, than in terms of age of the first estrus, an index of ovulation and attainment of fertility, suggesting that perturbed astrocyte function caused by *Kiss1r* ablation is possibly more relevant in terms of pubertal activation rather than completion. Female G-KiRKO mice also displayed alterations of estrous cyclicity under HFD conditions, with longer cycles and shorter periods at the ovulatory phase, estrus; a phenomenon that was not detected under normal feeding. Similarly, HFD aggravated the changes in LH pulsatility observed in G-KiRKO mice. Altogether, these findings strongly suggest that females devoid of kisspeptin signaling in astrocytes are more susceptive to the deleterious effects of HFD on adult gonadotropic axis. Considering the suspected dual impact of obesity on Kiss1 neurons (3), with initial over-activation followed by long-term suppression, our data suggest that this astrocyte regulatory circuit, parallel to the direct effects of kisspeptins on GnRH neurons, contributes to

460 adaptative responses of the reproductive axis to obesogenic stressors, both during puberty and
461 adulthood, mainly in females.

462 In terms of metabolic profiles, male and female G-KiRKO mice failed to show overt differences in adult
463 body weight or composition vs. control animals fed either a normal diet or HFD. However, G-KiRKO mice
464 displayed modestly improved glycemic responses to glucose overload, without consistent changes in
465 insulin sensitivity. This observation suggests that kisspeptin signaling in astrocytes may participate in the
466 control of glucose homeostasis, with a predicted function as a factor favoring (modest) glucose intolerance.
467 While the mechanisms for such phenomenon are yet to be clarified, this putative function appears to be
468 more evident in males than in females, as in males fed a chow diet, the integral GTT responses were
469 significantly diminished, as index of improved glucose tolerance; similar trends were detected in G-KiRKO
470 males fed HFD. Opposite alterations, namely, a worsening of glucose tolerance, have been reported in
471 mice with conditional ablation of insulin receptors in GFAP-expressing cells (58), suggesting an opposite
472 role of insulin vs. kisspeptin signaling in astrocytes in the control of peripheral glucose homeostasis.

473 In the last decades, the pivotal role of glial cells, and particularly of astrocytes, in the central modulation
474 of reproductive function has been defined, with a prominent role in the neurohormonal regulation of GnRH
475 neurosecretion. In addition, insulin has been recently shown to target astrocytes to putatively modulate
476 GnRH neurons, and thereby puberty onset and gonadal function (20). A recent report has documented,
477 using pharmacogenomics, that global activation of GFAP-positive cells in the vicinity of GnRH neurons
478 stimulated GnRH neuronal firing and LH secretion (59), therefore confirming the prominent functional role
479 of astrocytes in GnRH control. Our present data disclose an additional, previously unnoticed regulatory
480 pathway, involving direct kisspeptin actions in astrocytes, that is likely to operate as self-restrain
481 mechanism for the potent releasing effect of kisspeptins on GnRH secretion, relevant for shaping pulsatile
482 GnRH secretion (see **Figure 6B**). This non-neuronal signaling pathway of kisspeptins in the brain may
483 also mediate at least part of the adaptative reproductive responses to metabolic stressors, as an
484 obesogenic diet.

Methods

Detailed description of Methods can be found at **Supplemental Methods**.

Sex as biological variable. Studies were implemented in male and female mice to explore potential sex-related differences. Initial exploratory analyses were done in males, but based on sex differences found, more in-depth characterization of kisspeptin signaling in astrocytes was conducted in females.

Animals. Mice were housed in the Experimental Animal Service of the University of Córdoba, or animal facilities of the Universities of Cambridge or Lille. All animals were maintained at 12-h light/dark cycle, at standard temperature (22±2ºC) with ad libitum access to standard laboratory mice chow (A04, Panlab) and water, unless mentioned otherwise. The day the litters were born was considered postnatal day-1 (PND1); animals were weaned at PND23. For the diet-induced obesity studies, mice were fed from weaning onwards with high-fat diet (HFD, ref#D12331; Research Diets, New Brunswick, NJ) with 58%, 17%, and 25% calories from fat, protein and carbohydrate, respectively.

Experimental designs

Hypothalamic proteomic profiles after acute central administration of Kp-10 in Kiss1 KO mice. We conducted proteomic analyses of hypothalamic (POA) tissues of adult Kiss1 KO mice (n=9) after icv injection of an effective dose of Kp-10 (50 pmol). Adult Kiss1 KO male mice (n=6) icv injected with vehicle (Veh; 0.9% saline) served as controls. To avoid the potential confounding factor of kisspeptin-induced changes in testosterone levels, mice were orchidectomized 3 weeks before Kp-10 injection. Animals were euthanized 60 min after Kp-10 administration, and POA was excised and processed for proteomic determinations (nano-HPLC associated to triple-TOP equipped with SWATH acquisition or 2-DIGE).

Effect of acute central administration of Kp-10 on astrocyte glial markers in Kiss1 KO mice. RT-qPCR and Western blot analyses were performed to assess the effect of central Kp-10 injection on the astroglial markers, GFAP and vimentin. Adult Kiss1 KO male mice were icv injected with Kp-10 or Veh (n=3-4/group). After 60 min, animals were euthanized and POA was excised and processed for analysis.

Kiss1r expression in primary astrocyte cultures and functional studies. To assess whether *Kiss1r* is expressed in astrocytes and, subsequently, whether it is functional, primary astrocyte cultures from the hypothalamus of neonatal rats and mice were generated. *Kiss1r* expression was assessed by RT-qPCR, which was also applied to human astrocyte cultures. Once expression of *Kiss1r* was demonstrated, we conducted functional studies. Astrocyte cultures from neonatal rats were incubated with Kp-10 or vehicle (Veh) at different times (1, 10 and 30 min). Functional studies were conducted also in astrocyte cultures from neonatal mice, incubated during 10 min with Kp-10, based on our results from rat cultures. Cortical

astrocyte cultures were also included to compare effects in astrocytes from different brain locations. Mouse astrocyte cultures were also incubated with epidermal grown factor (EGF; 50 ng/ml, Gibco), as positive control (60). Finally, astrocyte cultures from G-KiRKO mice were incubated with Kp-10 (10^{-8} M), at 1- and 10-min. Astrocyte cultures from control mice were used as positive control.

Co-localization of Kiss1r and GFAP/S100β in mouse brain and Kiss1r expression in isolated astrocytes. To evaluate the astrocyte expression of *Kiss1r* in vivo, we first used RNAscope, to combine RNA *in situ* hybridization (ISH) with immunofluorescence (the latter, for GFAP and S100β detection, as canonical astrocyte markers). Brain sections from 4 adult female control mice at diestrus were incubated with the probes for *Kiss1r* (revealed in green) and *GnRH* (revealed in far red). Thereafter, immunohistochemical detection of GFAP (revealed in cyan) and S100β (revealed in magenta) was performed. For each animal, two slides were taken: one covering the OVLT and AVPV, and the second including the ARC and cortex. In parallel, astrocytes were isolated from the POA, MBH and cortex from adult male (n=6) and female (n=6) mice, using FACS, and *Kiss1r* expression was assessed by qPCR.

Assessment of appositions between GFAP-positive astrocytes and Kiss1 and GnRH neurons. Double immunohistochemical analyses were conducted in diestrus female mice (n=2) for assessing whether there are close appositions between Kiss1 neurons (revealed in magenta) and GFAP-expressing astrocytes (revealed in green) in the ARC and AVPV. In addition, triple immunofluorescence detection was conducted in cyclic control female mice to interrogate the intimate appositions between Kiss1 and GnRH neurons with GFAP-expressing astrocytes across the estrous cycle.

Phenotypic evaluation of sexual maturation, estrous cyclicity and fertility in adult G-KiRKO mice. Three-week-old control male (n=20) and female (n=16) mice, and age-paired G-KiRKO male (n=12) and female (n=16) mice, were checked for phenotypic markers of puberty (61). In adulthood, control (n=7) and G-KiRKO (n=11) female mice were monitored daily to assess estrous cyclicity. Virgin control (n=4) and G-KiRKO (n=5) mice were crossed with control males to assess fertility rates and breeding intervals.

Pharmacological studies in adult G-KiRKO mice. LH responses to Kp-10 were studied in both G-KiRKO male (n=8) and female (n=5) mice. Control (males, n=4; females, n=10) and G-KiRKO mice of both sexes were icv injected with Kp-10 (50 pmol). Blood samples were collected before (basal) and 15, 30 and 60 minutes after injection.

Assessment of pulsatile and surge LH secretion in G-KiRKO female mice. Assessment of pulsatile LH secretion was conducted in control (n=10) and G-KiRKO (n=5) female mice. The LH surge profiles were analyzed also in control (n= 5) and G-KiRKO (n= 3) female mice, as described in Supplemental Methods.

Activation of GnRH neurons & astrocyte appositions after kisspeptin stimulation in G-KiRKO mice. To evaluate whether the lack of kisspeptin signaling alters astrocyte appositions to GnRH neurons and/or their activation following kisspeptin stimulation, adult control (n=5) and G-KiRKO (n=5) female mice at diestrus were ip injected with an effective dose of Kp-54 (1 nmol). Activation of GnRH neurons was assessed by immunohistochemical detection of cFos, in line with previous references showing higher efficiency of Kp-54 to induce cFos expression (30). In addition, double immunohistochemistry was applied to label GFAP and GnRH signals in the brains of these animals.

Analysis of metabolic and reproductive phenotypes of G-KiRKO mice after HFD. G-KiRKO mice and their controls were fed HFD from weaning onwards, for generation of diet-induced obesity. Three-week-old male (n=35) and female (n=16) controls, as well as G-KiRKO male (n=17) and female (n=9) mice fed HFD were checked for phenotypic markers of puberty on a daily basis, as described for mice fed chow diet. Adult virgin control (n=7) and G-KiRKO (n=7) female mice, fed HFD, were monitored daily for at least 3-4 weeks to characterize estrous cyclicity. In addition, adult male (n=9) and female (n=13) controls and male (n=14) and female (n=10) G-KiRKO mice on HFD were icv injected with Kp-10 (50 pmol) and LH secretory responses were monitored. Additional groups of control (n=6) and G-KiRKO (n=8) female mice, fed HFD for two-months, were subjected to analysis of LH pulsatility. Body composition analyses were also conducted in adult (4-mo-old) male (n=20) and female (n=10) controls, and male (n=13) and female (n=6) G-KiRKO mice, fed HFD. Finally, GTT and ITT were conducted in adult male (n=10) and female (n=10) controls and male (n=10) and female (n=9-10) G-KiRKO mice, fed HFD.

Gene expression analyses in primary astrocyte cultures from G-KiRKO mice. To evaluate whether ablation of *Kiss1r* in astrocytes alters the expression of key elements in astrocyte physiology, gene expression analyses were applied to primary cultures of astrocytes from control and G-KiRKO mice. The genes analyzed and their corresponding functional pathways are as follows: *Sox-2*, *Nanog* (progenitor and differentiation markers); *Ki67*, *Cdk2* (cell proliferation and migration); *Tspo*, *Star*, *P450scc*, *Hsd3b1*, *P450arom* (steroidogenic pathway factors); *SynCam1*, *Ncam1* (cell adhesion and glia-to-GnRH neuron interaction factors); and *Cox-1*, *Cox-2*, *mPges*, *Pges-2* and *cPges* (prostaglandin synthesis pathway).

Statistical analyses. Statistical analyses were performed using Prism software (GraphPad Prism). All data are presented as mean ± standard error of the mean (SEM). Group sizes are denoted in the Methods section and/or figure legends for each experiment. Sample sizes were defined in line our previous experience in experimental studies using rodent species to evaluate the neuroendocrine regulation of puberty and adult reproductive function (62), assisted by previous a priori power analyses using dedicated software (e.g., GRANMO, https://apisal.es/Investigacion/Recursos/granmo.html) and values of standard

deviation that we usually obtain when measuring analogous parameters. These predictions defined that the selected sample sizes would provide at least 80% power to detect effect sizes using the tests indicated above, with a significance level of 0.05. Nonetheless, according to standard procedures, more complex molecular and histological analyses were implemented in representative subsets of randomly-assigned samples from each group. Unless otherwise stated, unpaired two-tailed Student's t-tests were applied for assessment of differences between two groups, while one- or two-way ANOVA (as indicated in figure legends) followed by post hoc Bonferroni tests were applied for comparisons of more than two groups. A P value less than 0.05 was considered significant, and different letters and/or asterisks have been used to indicate statistical significance. As general principle, the investigators directly performing animal experimentation and analyses were not blinded to the group allocation, but primary data analyses conducted by senior authors were conducted independently to avoid any potential bias.

Study Approvals. Unless otherwise stated, the experiments and animal protocols were approved by the Ethical Committee of the University of Córdoba and Junta de Andalusia; animal experiments were conducted in accordance with European Union normative for the use and care of experimental animals (EU Directive 2010/63/UE, September 2010). In addition, for experiments involving Kp-10 icv injection in Kiss1 KO mice, animals were killed in accordance with the UK Home Office regulations under the Animal (Scientific Procedures) Act of 1986. Establishment, breeding and care of this mouse line were approved by a Local Ethics Committee at Cambridge University and performed under authority of a Home Office License (UK). Finally, some of the studies, involving primary cultures of mouse astrocytes and RNAscope analyses in brain tissue sections and FACS isolation of mouse astrocytes, were conducted under approval of the Institutional Ethics Committee for the Care and Use of Experimental Animals of Lille University (APAFIS#2617-2015110517317420 v5). The studies on primary cultures of astrocytes from cortical and hypothalamic tissues micro-dissected from human fetuses were approved by the French Agency for Biomedical Research (France; protocol# PFS16-002).

Data availability. The authors declare that the data supporting the findings of this study are included in this article and its supplementary information files. All relevant source data are provided at the following DOI: http://dx.doi.org/10.12751/g-node. z9q4zs. Any additional information will be made available from the corresponding authors, upon request.

608 **Authors contributions**

609 ET: experimental studies, primary analysis and evaluation of data, draft of figures and manuscript; GP:
610 RNAscope and immunohistochemical analyses, with the assistance of AC-R; MG-R: in vivo experiments,
611 incl. characterization of G-KiRKO mice and LH pulsatility, with assistance of CP-L and SL; ACF-F:
612 astrocyte cultures from G-KiRKO mice, gene expression analyses thereof; IV: generation of mouse
613 models and expression/functional studies; AL: optimization of FACS, gene expression analyses thereof;
614 T.L.H and F.N: conception/interpretation of triple labeling immunocytochemical studies, conducted by
615 M.S.; SHY and SMM: initial functional studies in Kiss1 KO mice and protein/RNA analyses; MJS-T, VMN
616 and RP: immunohistochemical analyses and protein analyses; JR: in vivo studies and discussion of data;
617 JA and JC: generation/analysis of rat astrocyte cultures and discussion of data; RML: astrocyte cultures
618 and gene expression thereof; AS and VP: design/implementation of mouse astrocyte cultures, RNAscope
619 and FACS, and discussion of data; WHC: Kiss1 KO studies and assistance in study design; MT-S and
620 AR designed and co-supervised the whole study, analyzed and discussed the data. AR had leading roles
621 in proteomic analyses, while MTS was project-leader and senior responsible for final preparation of the
622 manuscript. All authors take full responsibility of the work. MT-S and AR are both senior/corresponding
623 authors of this study.

624 **Competing Interests' Statement**

625 The authors declare no competing interests with the contents of this work.

626 **Acknowledgements**

627 Supported by grants BFU2017-83934-P, PID2020-118660GB-I00 (MT-S), and PID2019-105564RB-I00
628 (RML), from Agencia Estatal Investigación, Spain; co-funded with EU-funds from FEDER Program;
629 project PIE14-00005 (MT-S, Instituto de Salud Carlos III, Spain); Project P18-RT-4093 (MT-S; Junta
630 Andalucía, Spain), Project 1254821 (MT-S; Univ. Córdoba-FEDER); BBSRC Project Grant, BB/K003178/1
631 (WHC), and EU-research contracts 659474 (WHM/ARR) and GAP-2014-655232 (MT-S). CIBER is an
632 initiative of Instituto de Salud Carlos III. The authors are indebted with Drs. Ignacio Ortea and Eduardo
633 Chicano (Proteomics Unit of IMIBIC), for their superb assistance. IMIBIC is part of the Biomodel-Platform
634 of Instituto de Salud Carlos III.
635

References

1. Herbison AE. Control of puberty onset and fertility by gonadotropin-releasing hormone neurons. *Nat Rev Endocrinol.* 2016;12(8):452-66.
2. Maeda K, Ohkura S, Uenoyama Y, Wakabayashi Y, Oka Y, Tsukamura H, et al. Neurobiological mechanisms underlying GnRH pulse generation by the hypothalamus. *Brain Res.* 2010;1364:103-15.
3. Sobrino V, Avendano MS, Perdices-Lopez C, Jimenez-Puyer M, and Tena-Sempere M. Kisspeptins and the neuroendocrine control of reproduction: Recent progress and new frontiers in kisspeptin research. *Front Neuroendocrinol.* 2022;65:100977.
4. Kirilov M, Clarkson J, Liu X, Roa J, Campos P, Porteous R, et al. Dependence of fertility on kisspeptin-Gpr54 signaling at the GnRH neuron. *Nat Commun.* 2013;4:2492.
5. Novaira HJ, Sonko ML, Hoffman G, Koo Y, Ko C, Wolfe A, et al. Disrupted kisspeptin signaling in GnRH neurons leads to hypogonadotrophic hypogonadism. *Mol Endocrinol.* 2014;28(2):225-38.
6. Leon S, Barroso A, Vazquez MJ, Garcia-Galiano D, Manfredi-Lozano M, Ruiz-Pino F, et al. Direct Actions of Kisspeptins on GnRH Neurons Permit Attainment of Fertility but are Insufficient to Fully Preserve Gonadotropic Axis Activity. *Sci Rep.* 2016;6:19206.
7. Clarkson J, Han SY, Piet R, McLennan T, Kane GM, Ng J, et al. Definition of the hypothalamic GnRH pulse generator in mice. *Proc Natl Acad Sci U S A.* 2017;114(47):E10216-E23.
8. Garcia-Galiano D, Pinilla L, and Tena-Sempere M. Sex steroids and the control of the Kiss1 system: developmental roles and major regulatory actions. *J Neuroendocrinol.* 2012;24(1):22-33.
9. Yeo SH, and Herbison AE. Projections of arcuate nucleus and rostral periventricular kisspeptin neurons in the adult female mouse brain. *Endocrinology.* 2011;152(6):2387-99.
10. Liu X, Yeo SH, McQuillan HJ, Herde MK, Hessler S, Cheong I, et al. Highly redundant neuropeptide volume co-transmission underlying episodic activation of the GnRH neuron dendron. *Elife.* 2021;10.
11. Ojeda SR, Lomniczi A, and Sandau US. Glial-gonadotrophin hormone (GnRH) neurone interactions in the median eminence and the control of GnRH secretion. *J Neuroendocrinol.* 2008;20(6):732-42.
12. Clasadonte J, and Prevot V. The special relationship: glia-neuron interactions in the neuroendocrine hypothalamus. *Nat Rev Endocrinol.* 2018;14(1):25-44.
13. Pellegrino G, Martin M, Allet C, Lhomme T, Geller S, Franssen D, et al. GnRH neurons recruit astrocytes in infancy to facilitate network integration and sexual maturation. *Nat Neurosci.* 2021;24(12):1660-72.
14. Baroncini M, Allet C, Leroy D, Beauvillain JC, Francke JP, and Prevot V. Morphological evidence for direct interaction between gonadotrophin-releasing hormone neurones and astroglial cells in the human hypothalamus. *J Neuroendocrinol.* 2007;19(9):691-702.
15. Garcia-Segura LM, Lorenz B, and DonCarlos LL. The role of glia in the hypothalamus: implications for gonadal steroid feedback and reproductive neuroendocrine output. *Reproduction.* 2008;135(4):419-29.
16. Rage F, Lee BJ, Ma YJ, and Ojeda SR. Estradiol enhances prostaglandin E2 receptor gene expression in luteinizing hormone-releasing hormone (LHRH) neurons and facilitates the LHRH response to PGE2 by activating a glia-to-neuron signaling pathway. *J Neurosci.* 1997;17(23):9145-56.
17. Clasadonte J, Poulain P, Hanchate NK, Corfas G, Ojeda SR, and Prevot V. Prostaglandin E2 release from astrocytes triggers gonadotropin-releasing hormone (GnRH) neuron firing via EP2 receptor activation. *Proc Natl Acad Sci U S A.* 2011;108(38):16104-9.
18. Fuente-Martin E, Garcia-Caceres C, Granado M, de Ceballos ML, Sanchez-Garrido MA, Sarman B, et al. Leptin regulates glutamate and glucose transporters in hypothalamic astrocytes. *J Clin Invest.* 2012;122(11):3900-13.
19. Varela L, Stutz B, Song JE, Kim JG, Liu ZW, Gao XB, et al. Hunger-promoting AgRP neurons trigger an astrocyte-mediated feed-forward autoactivation loop in mice. *J Clin Invest.* 2021;131(10).
20. Manaserh IH, Chikkamenahalli L, Ravi S, Dube PR, Park JJ, and Hill JW. Ablating astrocyte insulin receptors leads to delayed puberty and hypogonadism in mice. *PLoS Biol.* 2019;17(3):e3000189.
21. d'Anglemont de Tassigny X, Fagg LA, Dixon JP, Day K, Leitch HG, Hendrick AG, et al. Hypogonadotropic hypogonadism in mice lacking a functional Kiss1 gene. *Proc Natl Acad Sci U S A.* 2007;104(25):10714-9.
22. Navarro VM, Castellano JM, Fernandez-Fernandez R, Tovar S, Roa J, Mayen A, et al. Characterization of the potent luteinizing hormone-releasing activity of KiSS-1 peptide, the natural ligand of GPR54. *Endocrinology.* 2005;146(1):156-63.
23. Middeldorp J, and Hol EM. GFAP in health and disease. *Prog Neurobiol.* 2011;93(3):421-43.
24. Pinilla L, Aguilar E, Dieguez C, Millar RP, and Tena-Sempere M. Kisspeptins and reproduction: physiological roles and regulatory mechanisms. *Physiol Rev.* 2012;92(3):1235-316.

25. Irwig MS, Fraley GS, Smith JT, Acohido BV, Popa SM, Cunningham MJ, et al. Kisspeptin activation of gonadotropin releasing hormone neurons and regulation of KiSS-1 mRNA in the male rat. *Neuroendocrinology.* 2004;80(4):264-72.
26. Zhuo L, Theis M, Alvarez-Maya I, Brenner M, Willecke K, and Messing A. hGFAP-cre transgenic mice for manipulation of glial and neuronal function in vivo. *Genesis.* 2001;31(2):85-94.
27. Garcia-Galiano D, van Ingen Schenau D, Leon S, Krajnc-Franken MA, Manfredi-Lozano M, Romero-Ruiz A, et al. Kisspeptin signaling is indispensable for neurokinin B, but not glutamate, stimulation of gonadotropin secretion in mice. *Endocrinology.* 2012;153(1):316-28.
28. Ruohonen ST, Gaytan F, Usseglio Gaudi A, Velasco I, Kukoricza K, Perdices-Lopez C, et al. Selective loss of kisspeptin signaling in oocytes causes progressive premature ovulatory failure. *Hum Reprod.* 2022;37(4):806-21.
29. Davidoff MS, Middendorff R, Kofuncu E, Muller D, Jezek D, and Holstein AF. Leydig cells of the human testis possess astrocyte and oligodendrocyte marker molecules. *Acta Histochem.* 2002;104(1):39-49.
30. d'Anglemont de Tassigny X, Jayasena CN, Murphy KG, Dhillo WS, and Colledge WH. Mechanistic insights into the more potent effect of KP-54 compared to KP-10 in vivo. *PLoS One.* 2017;12(5):e0176821.
31. Chen C, Zhong X, Smith DK, Tai W, Yang J, Zou Y, et al. Astrocyte-Specific Deletion of Sox2 Promotes Functional Recovery After Traumatic Brain Injury. *Cereb Cortex.* 2019;29(1):54-69.
32. Ding Z, Dai C, Shan W, Liu R, Lu W, Gao W, et al. TNF-alpha up-regulates Nanog by activating NF-kappaB pathway to induce primary rat spinal cord astrocytes dedifferentiation. *Life Sci.* 2021;287:120126.
33. Kang W, Balordi F, Su N, Chen L, Fishell G, and Hebert JM. Astrocyte activation is suppressed in both normal and injured brain by FGF signaling. *Proc Natl Acad Sci U S A.* 2014;111(29):E2987-95.
34. Tikoo R, Casaccia-Bonnefil P, Chao MV, and Koff A. Changes in cyclin-dependent kinase 2 and p27kip1 accompany glial cell differentiation of central glia-4 cells. *J Biol Chem.* 1997;272(1):442-7.
35. Lavaque E, Sierra A, Azcoitia I, and Garcia-Segura LM. Steroidogenic acute regulatory protein in the brain. *Neuroscience.* 2006;138(3):741-7.
36. Sandau US, Mungenast AE, McCarthy J, Biederer T, Corfas G, and Ojeda SR. The synaptic cell adhesion molecule, SynCAM1, mediates astrocyte-to-astrocyte and astrocyte-to-GnRH neuron adhesiveness in the mouse hypothalamus. *Endocrinology.* 2011;152(6):2353-63.
37. Sampey AV, Monrad S, and Crofford LJ. Microsomal prostaglandin E synthase-1: the inducible synthase for prostaglandin E2. *Arthritis Res Ther.* 2005;7(3):114-7.
38. Lee SJ, Seo BR, and Koh JY. Metallothionein-3 modulates the amyloid beta endocytosis of astrocytes through its effects on actin polymerization. *Mol Brain.* 2015;8(1):84.
39. Banati RB, Gehrmann J, Wiessner C, Hossmann KA, and Kreutzberg GW. Glial expression of the beta-amyloid precursor protein (APP) in global ischemia. *J Cereb Blood Flow Metab.* 1995;15(4):647-54.
40. O'Leary LA, Davoli MA, Belliveau C, Tanti A, Ma JC, Farmer WT, et al. Characterization of Vimentin-Immunoreactive Astrocytes in the Human Brain. *Front Neuroanat.* 2020;14:31.
41. Sharif A, Baroncini M, and Prevot V. Role of glia in the regulation of gonadotropin-releasing hormone neuronal activity and secretion. *Neuroendocrinology.* 2013;98(1):1-15.
42. Lange SC, Bak LK, Waagepetersen HS, Schousboe A, and Norenberg MD. Primary cultures of astrocytes: their value in understanding astrocytes in health and disease. *Neurochem Res.* 2012;37(11):2569-88.
43. Malatesta P, Hack MA, Hartfuss E, Kettenmann H, Klinkert W, Kirchhoff F, et al. Neuronal or glial progeny: regional differences in radial glia fate. *Neuron.* 2003;37(5):751-64.
44. Tan Z, Liu Y, Xi W, Lou HF, Zhu L, Guo Z, et al. Glia-derived ATP inversely regulates excitability of pyramidal and CCK-positive neurons. *Nat Commun.* 2017;8:13772.
45. Cheung G, Bataveljic D, Visser J, Kumar N, Moulard J, Dallerac G, et al. Physiological synaptic activity and recognition memory require astroglial glutamine. *Nat Commun.* 2022;13(1):753.
46. Fernandez-Gayol O, Sanchis P, Aguilar K, Navarro-Sempere A, Comes G, Molinero A, et al. Different Responses to a High-Fat Diet in IL-6 Conditional Knockout Mice Driven by Constitutive GFAP-Cre and Synapsin 1-Cre Expression. *Neuroendocrinology.* 2019;109(2):113-30.
47. Manfredi-Lozano M, Roa J, Ruiz-Pino F, Piet R, Garcia-Galiano D, Pineda R, et al. Defining a novel leptin-melanocortin-kisspeptin pathway involved in the metabolic control of puberty. *Mol Metab.* 2016;5(10):844-57.
48. Font-Nieves M, Sans-Fons MG, Gorina R, Bonfill-Teixidor E, Salas-Perdomo A, Marquez-Kisinousky L, et al. Induction of COX-2 enzyme and down-regulation of COX-1 expression by lipopolysaccharide (LPS) control prostaglandin E2 production in astrocytes. *J Biol Chem.* 2012;287(9):6454-68.

49. Forbes S, Li XF, Kinsey-Jones J, and O'Byrne K. Effects of ghrelin on Kisspeptin mRNA expression in the hypothalamic medial preoptic area and pulsatile luteinising hormone secretion in the female rat. *Neurosci Lett.* 2009;460(2):143-7.
50. Popa SM, Moriyama RM, Caligioni CS, Yang JJ, Cho CM, Concepcion TL, et al. Redundancy in Kiss1 expression safeguards reproduction in the mouse. *Endocrinology.* 2013;154(8):2784-94.
51. Sinchak K, Mohr MA, and Micevych PE. Hypothalamic Astrocyte Development and Physiology for Neuroprogesterone Induction of the Luteinizing Hormone Surge. *Front Endocrinol (Lausanne).* 2020;11:420.
52. Garcia-Caceres C, Balland E, Prevot V, Luquet S, Woods SC, Koch M, et al. Role of astrocytes, microglia, and tanycytes in brain control of systemic metabolism. *Nat Neurosci.* 2019;22(1):7-14.
53. Nampoothiri S, Nogueiras R, Schwaninger M, and Prevot V. Glial cells as integrators of peripheral and central signals in the regulation of energy homeostasis. *Nat Metab.* 2022;4(7):813-25.
54. Buckman LB, Thompson MM, Lippert RN, Blackwell TS, Yull FE, and Ellacott KL. Evidence for a novel functional role of astrocytes in the acute homeostatic response to high-fat diet intake in mice. *Mol Metab.* 2015;4(1):58-63.
55. Tena-Sempere M. Interaction between energy homeostasis and reproduction: central effects of leptin and ghrelin on the reproductive axis. *Horm Metab Res.* 2013;45(13):919-27.
56. Kim JG, Suyama S, Koch M, Jin S, Argente-Arizon P, Argente J, et al. Leptin signaling in astrocytes regulates hypothalamic neuronal circuits and feeding. *Nat Neurosci.* 2014;17(7):908-10.
57. Li XF, Lin YS, Kinsey-Jones JS, and O'Byrne KT. High-fat diet increases LH pulse frequency and kisspeptin-neurokinin B expression in puberty-advanced female rats. *Endocrinology.* 2012;153(9):4422-31.
58. Garcia-Caceres C, Quarta C, Varela L, Gao Y, Gruber T, Legutko B, et al. Astrocytic Insulin Signaling Couples Brain Glucose Uptake with Nutrient Availability. *Cell.* 2016;166(4):867-80.
59. Vanacker C, Defazio RA, Sykes CM, and Moenter SM. A role for glial fibrillary acidic protein (GFAP)-expressing cells in the regulation of gonadotropin-releasing hormone (GnRH) but not arcuate kisspeptin neuron output in male mice. *Elife.* 2021;10.
60. Martinez R, and Gomes FC. Neuritogenesis induced by thyroid hormone-treated astrocytes is mediated by epidermal growth factor/mitogen-activated protein kinase-phosphatidylinositol 3-kinase pathways and involves modulation of extracellular matrix proteins. *J Biol Chem.* 2002;277(51):49311-8.
61. Sanchez-Garrido MA, Castellano JM, Ruiz-Pino F, Garcia-Galiano D, Manfredi-Lozano M, Leon S, et al. Metabolic programming of puberty: sexually dimorphic responses to early nutritional challenges. *Endocrinology.* 2013;154(9):3387-400.
62. Vazquez MJ, Toro CA, Castellano JM, Ruiz-Pino F, Roa J, Beiroa D, et al. SIRT1 mediates obesity- and nutrient-dependent perturbation of pubertal timing by epigenetically controlling Kiss1 expression. *Nat Commun.* 2018;9(1):4194.

Legend to Figures

Figure 1: *Identification of kisspeptin targets in POA by proteomic analysis*. (**A**) Scheme of experimental design to identify new targets of kisspeptin actions in adult Kiss1 KO male mice (n=6 per group), using SWATH-MS method. (**B**) High-throughput data (77 differentially expressed proteins found) were analyzed via STRING, to build functional protein association networks (the three main clusters circled correspond to GO terms). Analyses were also implemented by (**C**) enrichment analyses in GO categories such as biological process visualized by Cytoscape platform; and (**D**) cellular components using *ggplot2* R package (cut-off r > ±0.800). In (**E**), box-plots represent the intensity of GFAP, APP and MT3 proteins from SWATH-MS raw data. Data are the mean±SEM. Statistical significance was determined by Student's t-test: *P<0.05 vs. corresponding values in adult Kiss1 KO mice treated with vehicle (Veh). (**F**) 2D-DIGE map (left panel) and pie chart (right panel) presenting the GO of enriched proteins from an independent validation of Kp-10 effects on Kiss1 KO mice. Red circles highlight differential protein expression in POA from Kiss1 KO mice after Kp-10 injection (n=3) vs. vehicle-treated mice (n=3). Spots were identified by MALDI-MS/MS.

Figure 2: *Evidence for kisspeptin signaling in astrocytes*. (**A**) Expression analysis of glial markers, *Gfap*/GFAP and *Vimentin*/Vimentin, at mRNA and protein levels, in POA of adult Kiss1 KO male mice after icv Kp-10 stimulation (n=3-4) vs. vehicle (n=3). Data are the mean±SEM. Statistical significance was determined by Student's t-test: *P<0.05 vs. KO mice treated with Veh. (**B**) Representative gels illustrating the expression of *Kiss1r*, but not *Kiss1* mRNA in two pools of primary astrocyte cultures from neonatal rat (upper gel) and mouse (lower gel) hypothalamus are presented. Hypothalamic (HTLA) tissue was used as positive control. MM, molecular markers. Real-time PCR of *Kiss1r* mRNA in primary mouse and human astrocyte cultures (n=4 for mouse; n=6 cortical and 5 hypothalamic human cultures) is also shown; values correspond to Ct data. The blue line represents the mean Ct value of the housekeeping gene. In (**C**), Western blots of phosphorylated ERK (pERK) and AKT (pAKT) in primary rat hypothalamic astrocytes are shown. Bar graphs show the effect of Kp-10 treatment (10^{-8} M; n=3) at 1-, 10- and 30-min (upper panel); representative blots are shown in the lower panel. Astrocyte cultures treated with vehicle (n=3) were used as a negative control. Data are the mean ± SEM. Statistical significance was determined by Student's t-test: **P <0.01 vs. astrocytes treated with vehicle. In (**D**), Western blots of pERK, total ERK (totERK), pAKT, total AKT (totAKT) and actin, in primary mouse cerebrocortical and hypothalamic astrocytes treated with Kp-10 (n=3) or Epidermal Growth Factor (EGF, 50 ng/ml; n=3), used as a positive control. Vehicle-treated astrocytes (n=3) were used as a negative controls. Data are the mean ± SEM.

Statistical significance was determined by 2-way ANOVA followed by Bonferroni's post-hoc test: ****P<0.0001, astrocytes treated with Kp-10 vs. vehicle; or cortical vs. hypothalamic astrocytes.

Figure 3: *Co-expression of Kiss1r in astrocytes and evidence for direct astrocyte-Kiss1 neuron interplay.* (**A-H**) Dual RNAscope ISH combined with immunohistochemistry in brain sections from diestrous female mice (n=4). (**A**) Representative image showing *Kiss1r* (green) mRNA and GFAP (cyan) and S100β (magenta) in the preoptic region. The magnified area (from dotted square in A) shows individual signals (**B**-**D**), while merge image documents co-expression of *Kiss1r* in GFAP/S100β-positive cells (arrowheads; **E**). In (**F**), representative image of *Kiss1r* (green) and *GnRH* (white) mRNA expression, and combined detection of astrocyte markers, GFAP and S100β proteins (magenta), in POA, including OVLT and AVPV. The magnified area (from dotted square in F) shows *Kiss1r* expression and neuronal nuclear labelling with DAPI (blue; **G**), while co-expression (arrowheads) of *Kiss1r* with *GnRH* and *Kiss1r* with astrocyte markers is shown in (**H**). (**I**) Percentage of GFAP/S100β-positive cells co-expressing *Kiss1r* mRNA in key hypothalamic areas, including ARC and AVPV, OVLT and cortex (CTX). Scale bar=100μm. Data are the mean±SEM. In (**J**-**K**), anatomical relationships between Kp-immunoreactive neurons and GFAP-positive astrocytes from diestrous female mice. Individual and merge images of Kp (magenta) and GFAP (green) are presented from AVPV (**J**) and ARC (**K**); 3D reconstructions of GFAP-immunoreactive astrocytes enwrapping cell bodies of Kp cells in AVPV are also shown (**J**); close appositions between GFAP-immunoreactive astrocytes and Kp-fibers are detected in ARC at high magnification (**K**). Scale bars=50 μm (J); 100μm (K). (**L**) Representative images of GnRH-neurons in close apposition with Kp-fibers are shown at the stages of the ovarian cycle (10:00 am); an additional image at proestrus afternoon is shown. Merge images of GnRH-neurons (green) and Kp-fibers (red) in the medial septal nucleus are presented. (**M**) Higher magnification of a representative image, with triple labeling of GnRH-neurons (green), Kp-fibers (blue) and GFAP-positive cells (red), in the hypothalamic medial septal nucleus.

Figure 4: *Kiss1r expression in astrocytes from adult mice isolated by FACS.* (**A**) Gating strategy for astrocyte isolation by FACS. The two plots in the left represent cells incubated with the control isotype; the two blots in the right represent cells incubated with the anti-ACSA-2-PE antibody. (**B**) Real-time PCR of astroglial [*Gfap, Glast, Connexin-43* (Cx43)], neuronal (*Elavl3, RBFox3*), microglial (*Aif1*) and endothelial (*CD31*) genes in FACS-sorted positive and negative fractions of the MBH of female mice, used for validation purposes. (**C**) Real-time PCR analysis of *Kiss1r* in FACS-sorted positive and negative fractions obtained from three brain areas [POA, MBH, and cortex (CTX)] of adult male and female (diestrus) mice. Expression data segregated by sex (females: left-panel; males: right-panel) are presented. Sex-aggregated data, divided per brain region, are displayed in **D**. N=6 animals per sex.

Values in the positive fraction are expressed relative to negative fraction values, set at 1. Data are the mean ± SEM. Statistical significance was determined by Student's t-test in **B**: *P<0.05; **P<0.01, vs. corresponding negative fraction; and by 2-way ANOVA followed by Bonferroni's post hoc test for regional and sex analyses in **C-D**: *P <0.05; **P<0.01 vs. negative fraction. Note that of the 36 positive fractions (3 regions x 2 sexes x 6 animals per group) tested**,** *Kiss1r* expression was readily detectable in 33, with a mean Ct value of 21.9.

Figure 5: *Characterization of reproductive phenotype of G-KiRKO female mice*. In upper panels, accumulated percentage of female mice displaying vaginal opening (VO; as pubertal marker) post-weaning, under normal diet (**A**) or HFD (**B**); mean ages of VO are presented as histograms. Group sizes: control (n=16); G-KiRKO (n=16); control-HFD (n=18); and G-KiRKO-HFD (n=9). Statistical significance for mean VO was assessed by Student's t-test (**A**) or one-way ANOVA followed by Bonferroni's test (**B**): ***P<0.001 vs. control mice. LH secretory responses, as 60-min profile after Kp-10 injection (50pmol), are shown for adult control and G-KiRKO female mice fed normal diet (**C**) or HFD (**D**); net increment of integral (AUC) LH secretion over 60-min period after Kp-10 is also presented. Group sizes: control (n=10); G-KiRKO (n=5); control-HFD (n=13); and G-KiRKO-HFD (n= 10). Statistical significance was determined by Student's t-test: *P<0.05 vs. control mice (AUC); and 2-way ANOVA followed by Bonferroni's test for time-course analyses: **/##P<0.01; ###P<0.001 and ****/####P<0.0001 vs. corresponding basal (time-0) values; and [a] P<0.05 G-KiRKO vs. control mice. (**E-F**) Graphs showing the percentual distribution of estrous cycle phases in control and G-KiRKO mice for normal diet (**E**) and HFD (**F**); control (n=7); G-KiRKO (n=12); control-HFD (n=7) and G-KiRKO-HFD (n=7). Mean duration of estrous cycle is displayed also. Statistical significance was determined by Student's t-test (**E**): **P<0.01 vs. control mice with normal diet; and by 2-way ANOVA followed by Bonferroni's test (**F**): **P<0.01; ***P<0.001 vs. control mice fed with HFD. (**G**) LH pulsatility parameters in G-KiRKO mice fed control diet are shown; control (n=9), G-KiRKO (n=6). Bar graphs showing basal LH, numbers of LH pulses (peaks), net increment (AUC) LH secretion and peak LH secretion over 3-h sampling are presented. (**H**) Similar parameters are shown for G-KiRKO mice under HFD: control (n=6), G-KiRKO (n=8). Student's t-test: *P<0.05; **P<0.01 vs. control mice.

Figure 6: *Gene expression profiling in G-KiRKO astrocyte primary cultures*. A comprehensive overview of the set of genes whose expression was analyzed by qPCR in astrocyte cultures of G-KiRKO mice is shown in the left panel. Gene categories correspond to astrocyte progenitors (purple), astrocyte proliferation (grey), cholesterol transport and steroidogenesis (yellow-brown), cell-cell adhesion interaction (red) and prostaglandin synthesis (blue). In the right panel, quantitative data from qPCR

877 expression analyses conducted in duplicate in individual astrocyte cultures from control (n=4) and G-
878 KiRKO (n=4) mice. The expression levels of *Sox-2*, *Nanog*, *Ki67*, *Cdk2*, *Tspo*, *Star*, *Hsd3b1*, *SynCam1*,
879 *Ncam1*, *Cox-1*, *Cox-2*, *mPges*, *Pges-2* and *cPges* mRNA are shown after normalization using *S11*
880 expression levels. Note that *P450scc* and *P450arom* displayed virtually undetectable expression levels
881 in our cultures, and hence are not presented in the histograms. Data are shown as mean±SEM. Statistical
882 significance was determined by Student's t-test: *P<0.05 vs. corresponding values in control astrocytes.

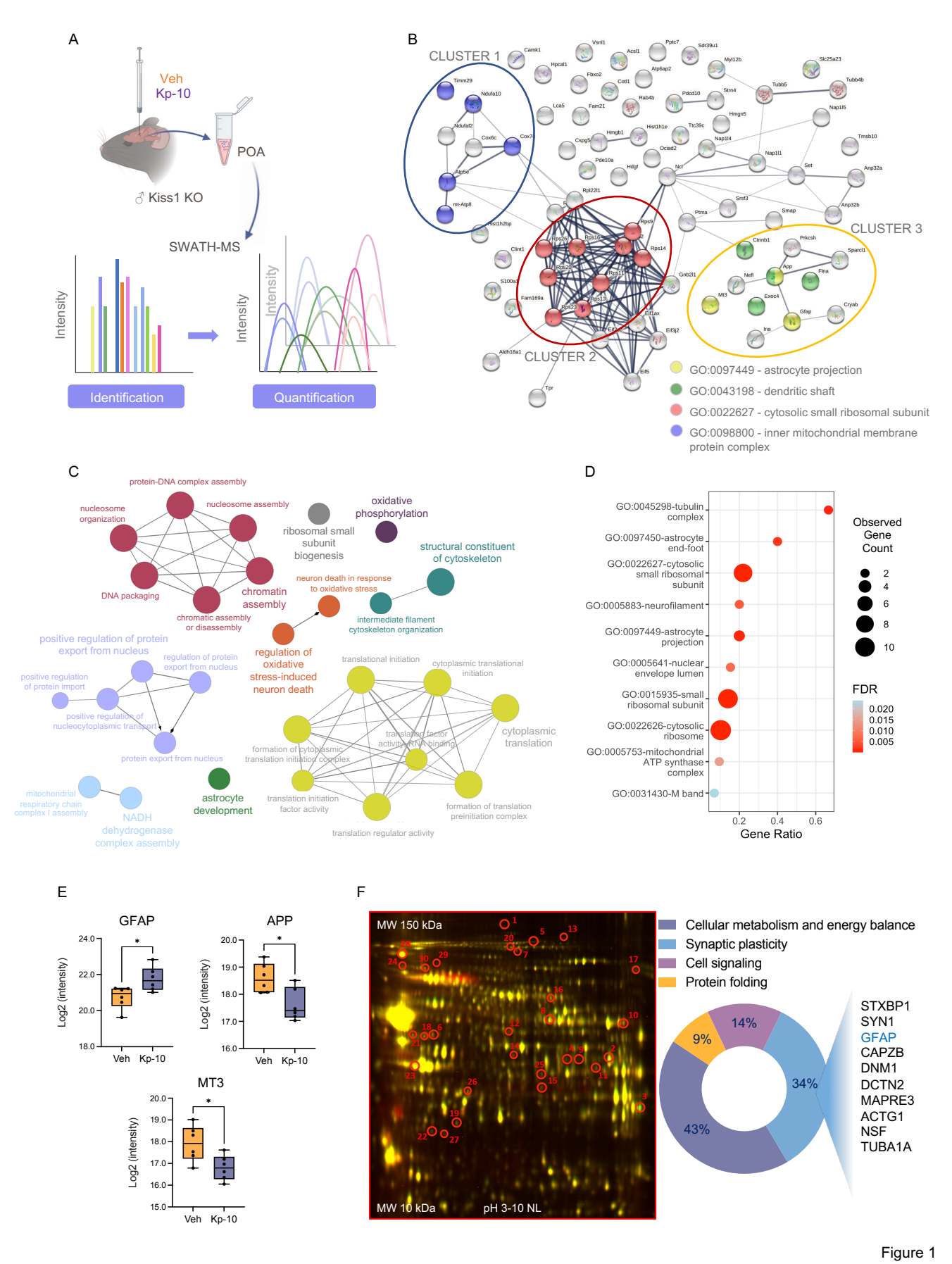
A
Veh
Kp-10
POA
♂ Kiss1 KO
SWATH-MS
Intensity
Intensity
Identification
Quantification
B
CLUSTER 1
CLUSTER 2
CLUSTER 3
GO:0097449 - astrocyte projection
GO:0043198 - dendritic shaft
GO:0022627 - cytosolic small ribosomal subunit
GO:0098800 - inner mitochondrial membrane protein complex
C
protein-DNA complex assembly
nucleosome organization
nucleosome assembly
DNA packaging
chromatin assembly
chromatic assembly or disassembly
ribosomal small subunit biogenesis
oxidative phosphorylation
structural constituent of cytoskeleton
neuron death in response to oxidative stress
intermediate filament cytoskeleton organization
regulation of oxidative stress-induced neuron death
positive regulation of protein export from nucleus
regulation of protein export from nucleus
positive regulation of protein import
positive regulation of nucleocytoplasmic transport
protein export from nucleus
translational initiation
cytoplasmic translational initiation
cytoplasmic translation
formation of cytoplasmic translation initiation complex
translation factor activity, RNA binding
translation initiation factor activity
formation of translation preinitiation complex
translation regulator activity
astrocyte development
mitochondrial respiratory chain complex I assembly
NADH dehydrogenase complex assembly
D
GO:0045298-tubulin complex
GO:0097450-astrocyte end-foot
GO:0022627-cytosolic small ribosomal subunit
GO:0005883-neurofilament
GO:0097449-astrocyte projection
GO:0005641-nuclear envelope lumen
GO:0015935-small ribosomal subunit
GO:0022626-cytosolic ribosome
GO:0005753-mitochondrial ATP synthase complex
GO:0031430-M band
Gene Ratio
Observed Gene Count
FDR
E
GFAP
APP
MT3
Log2 (intensity)
Veh
Kp-10
F
MW 150 kDa
MW 10 kDa
pH 3-10 NL
Cellular metabolism and energy balance
Synaptic plasticity
Cell signaling
Protein folding
14%
9%
34%
43%
STXBP1
SYN1
GFAP
CAPZB
DNM1
DCTN2
MAPRE3
ACTG1
NSF
TUBA1A

Figure 1

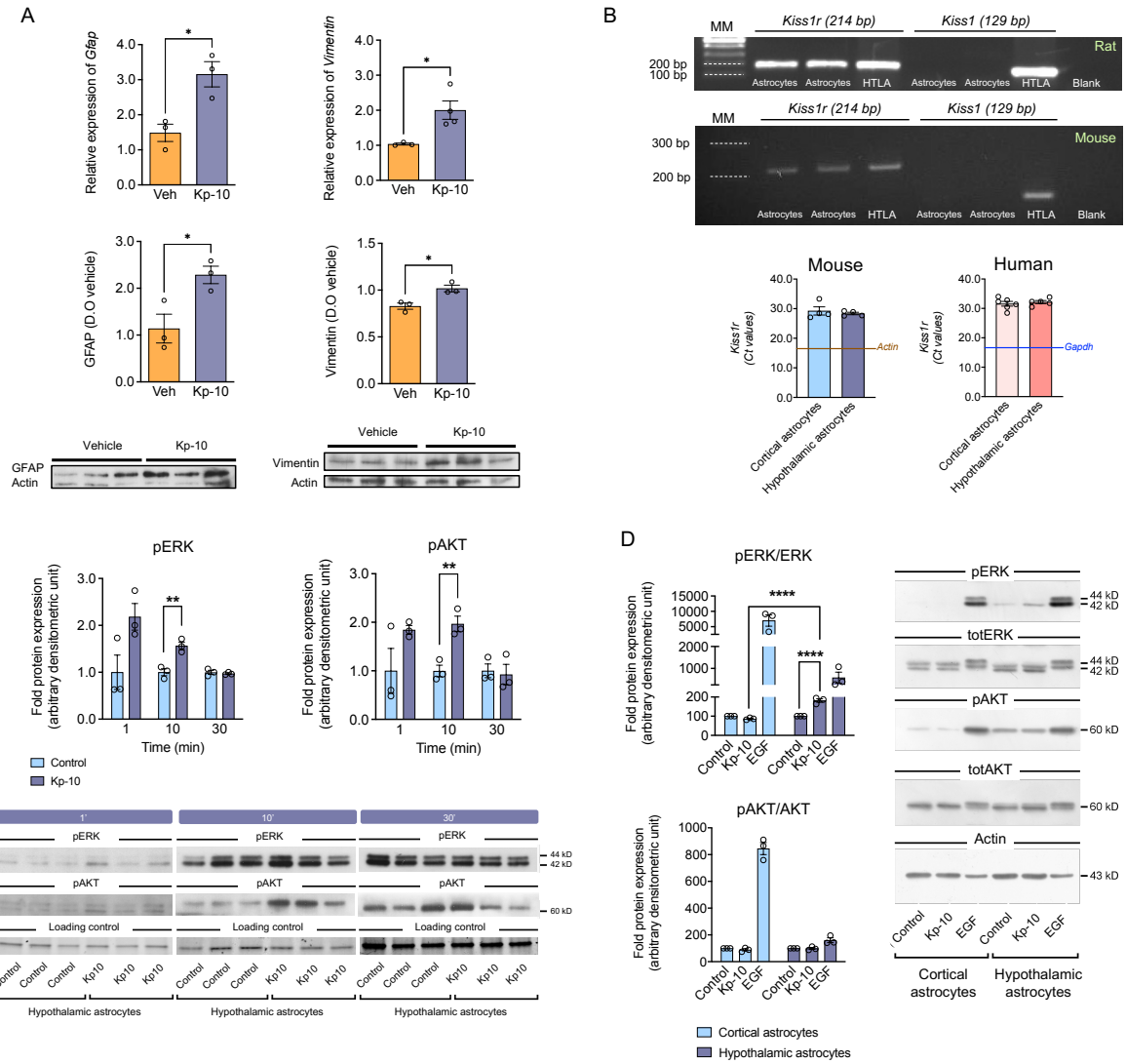
A
Relative expression of Gfap
Relative expression of Vimentin
GFAP (D.O vehicle)
Vimentin (D.O vehicle)
Veh
Kp-10
Vehicle
GFAP
Actin
Vimentin
B
MM
Kiss1r (214 bp)
Kiss1 (129 bp)
Rat
200 bp
100 bp
Astrocytes
HTLA
Blank
Mouse
300 bp
200 bp
Human
Kiss1r (Ct values)
Actin
Gapdh
Cortical astrocytes
Hypothalamic astrocytes
C
pERK
pAKT
Fold protein expression (arbitrary densitometric unit)
Time (min)
Control
Kp-10
Loading control
Hypothalamic astrocytes
D
pERK/ERK
pAKT/AKT
EGF
totERK
totAKT
Actin
Cortical astrocytes
Hypothalamic astrocytes
44 kD
42 kD
60 kD
43 kD

Figure 2

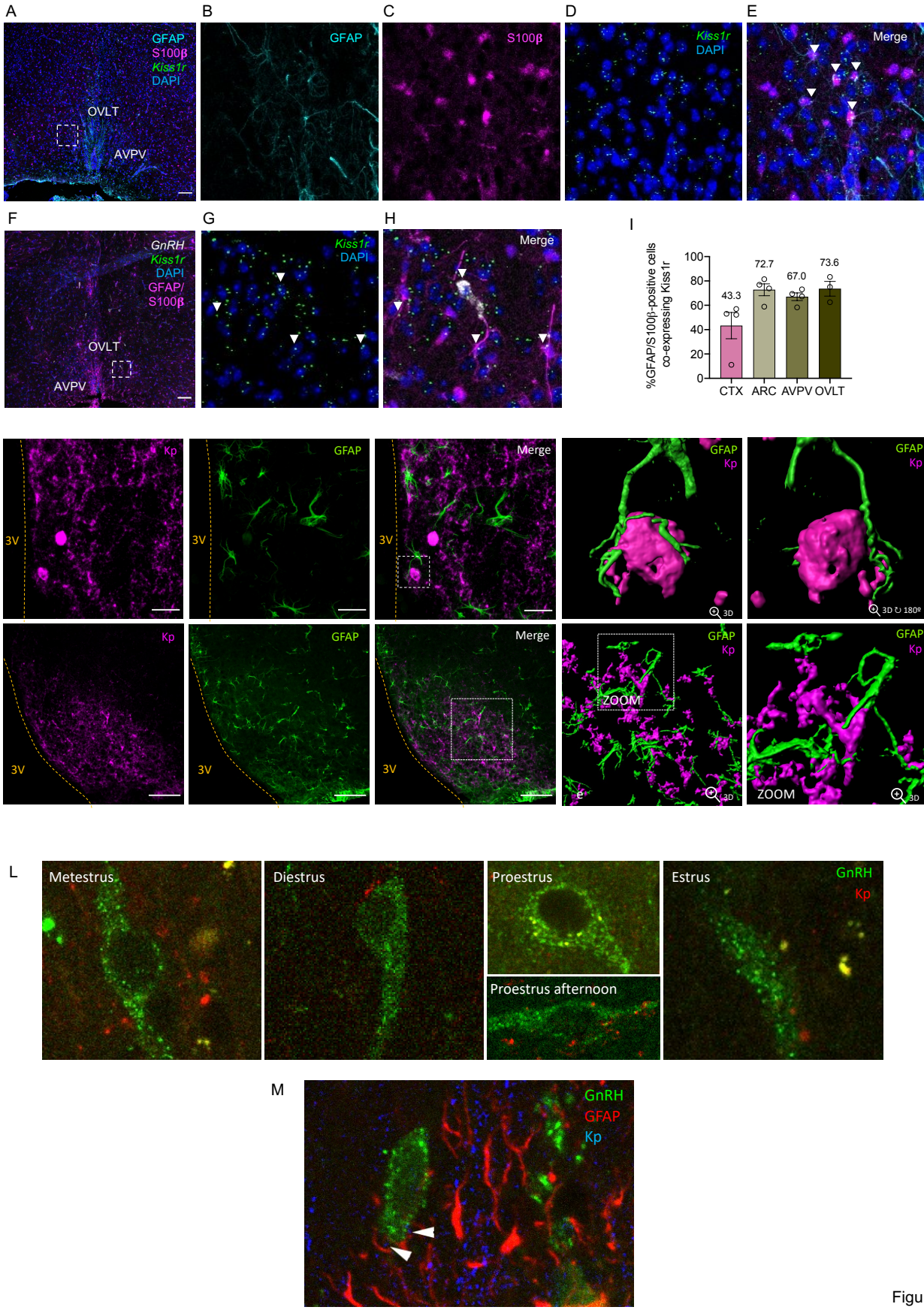
A
GFAP
S100β
Kiss1r
DAPI
OVLT
AVPV
B
GFAP
C
S100β
D
Kiss1r
DAPI
E
Merge
F
GnRH
Kiss1r
DAPI
GFAP/
S100β
OVLT
AVPV
G
Kiss1r
DAPI
H
Merge
I
%GFAP/S100β-positive cells co-expressing Kiss1r
100
80
60
40
20
0
43.3
72.7
67.0
73.6
CTX
ARC
AVPV
OVLT
J
Kp
3V
GFAP
Merge
3D
3D ↻ 180º
K
ZOOM
L
Metestrus
Diestrus
Proestrus
Proestrus afternoon
Estrus
GnRH
Kp
M
GnRH
GFAP
Kp

Figure 3

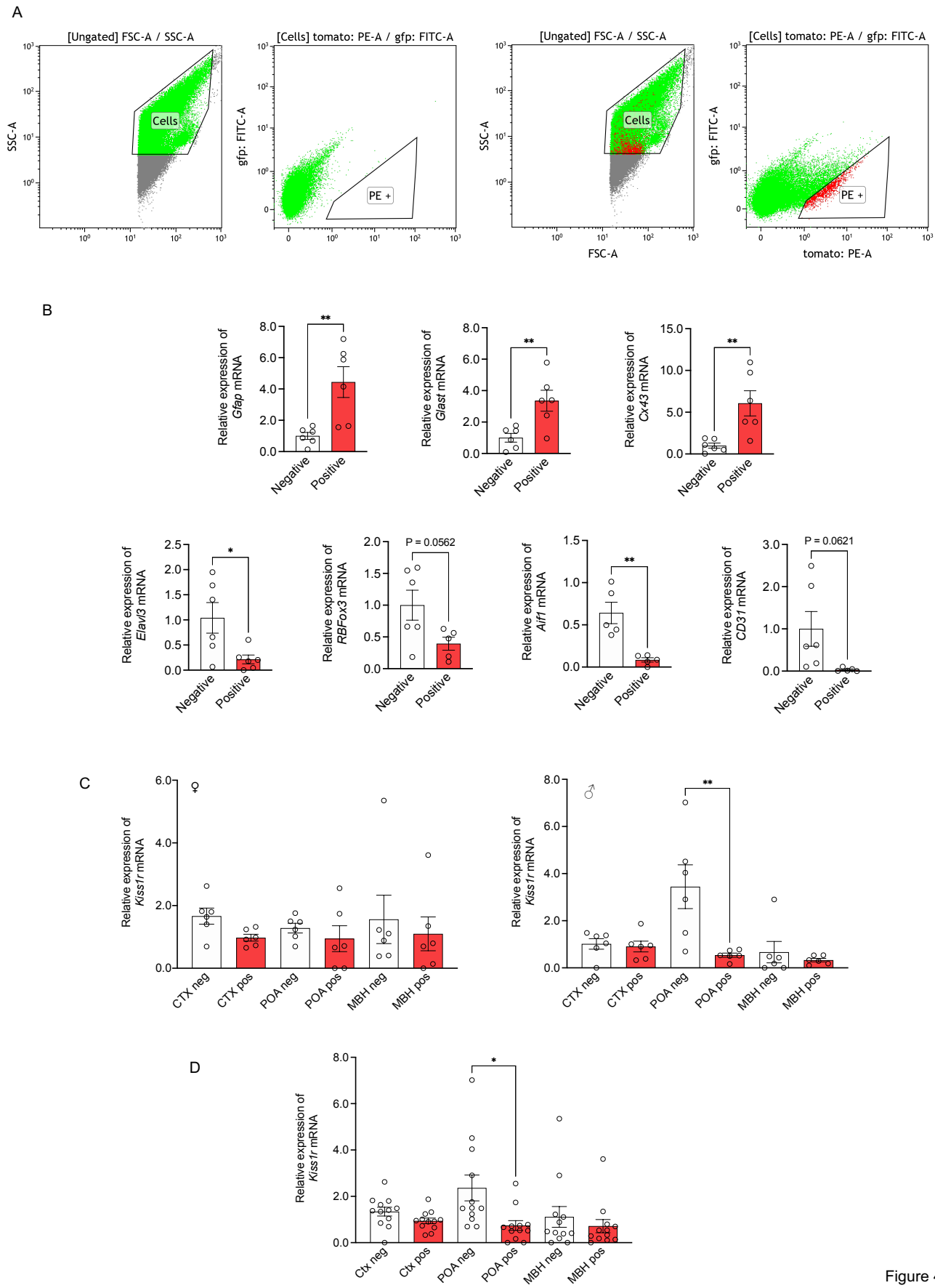
A
[Ungated] FSC-A / SSC-A
SSC-A
Cells
[Cells] tomato: PE-A / gfp: FITC-A
gfp: FITC-A
PE +
[Ungated] FSC-A / SSC-A
SSC-A
FSC-A
Cells
[Cells] tomato: PE-A / gfp: FITC-A
gfp: FITC-A
tomato: PE-A
PE +
B
Relative expression of Gfap mRNA
Relative expression of Glast mRNA
Relative expression of Cx43 mRNA
Relative expression of Elavl3 mRNA
Relative expression of RBFox3 mRNA
P = 0.0562
Relative expression of Aif1 mRNA
Relative expression of CD31 mRNA
P = 0.0621
Negative
Positive
C
Relative expression of Kiss1r mRNA
CTX neg
CTX pos
POA neg
POA pos
MBH neg
MBH pos
D
Relative expression of Kiss1r mRNA
Ctx neg
Ctx pos
POA neg
POA pos
MBH neg
MBH pos

Figure 4

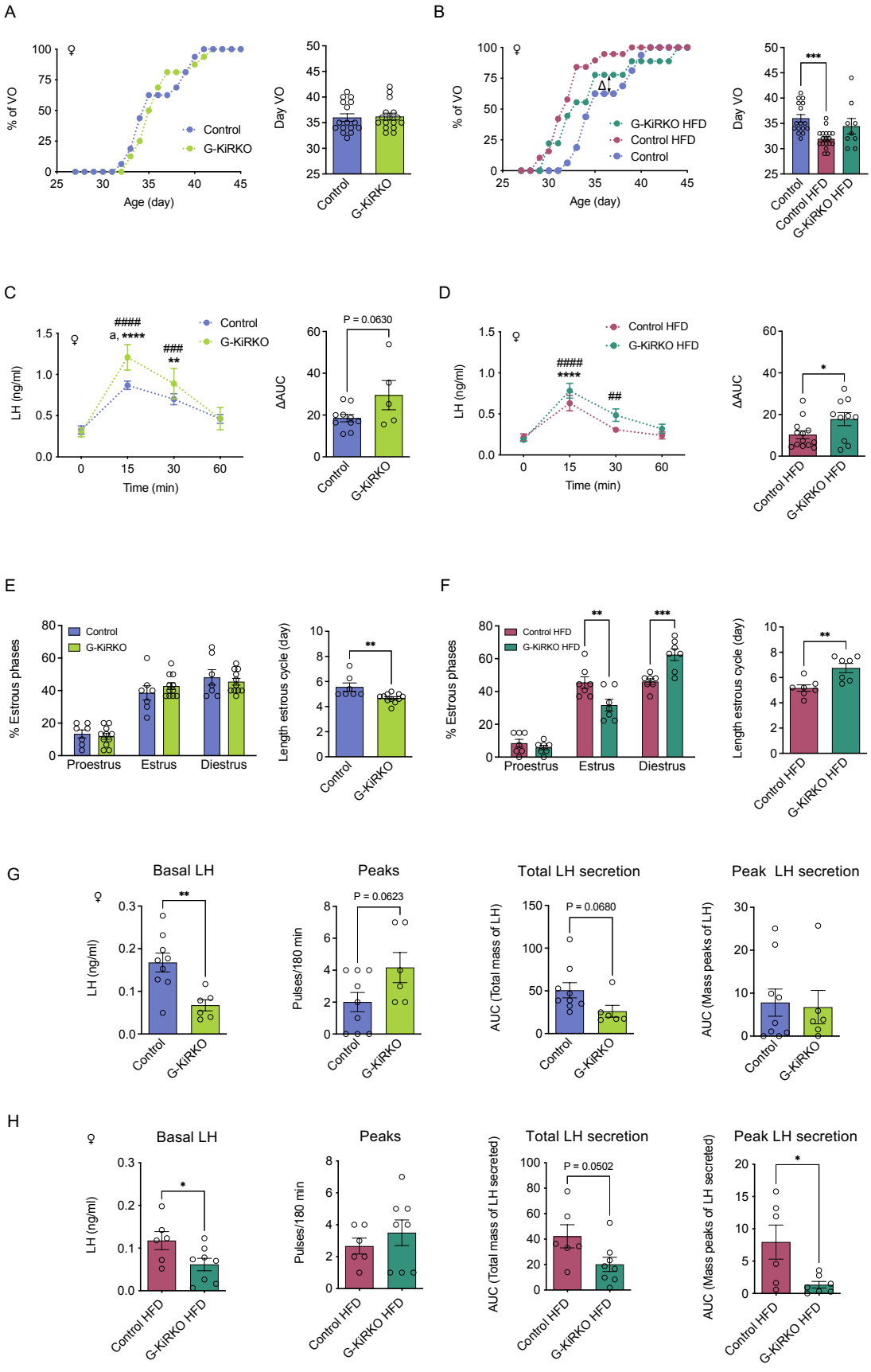
A
% of VO
Age (day)
Control
G-KiRKO
Day VO
B
G-KiRKO HFD
Control HFD
Control
***
C
LH (ng/ml)
Time (min)
####
a, ****
###
**
ΔAUC
P = 0.0630
D
##
*
E
% Estrous phases
Proestrus
Estrus
Diestrus
Length estrous cycle (day)
F
G
Basal LH
Peaks
Total LH secretion
Peak LH secretion
Pulses/180 min
AUC (Total mass of LH)
AUC (Mass peaks of LH)
P = 0.0623
P = 0.0680
H
AUC (Total mass of LH secreted)
AUC (Mass peaks of LH secreted)
P = 0.0502

Figure 5

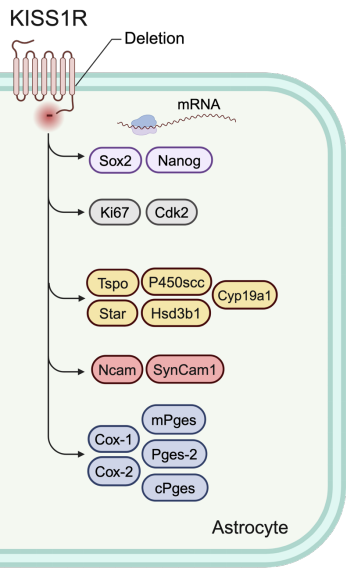
KISS1R
Deletion
mRNA
Sox2
Nanog
Ki67
Cdk2
Tspo
P450scc
Cyp19a1
Star
Hsd3b1
Ncam
SynCam1
mPges
Cox-1
Pges-2
Cox-2
cPges
Astrocyte

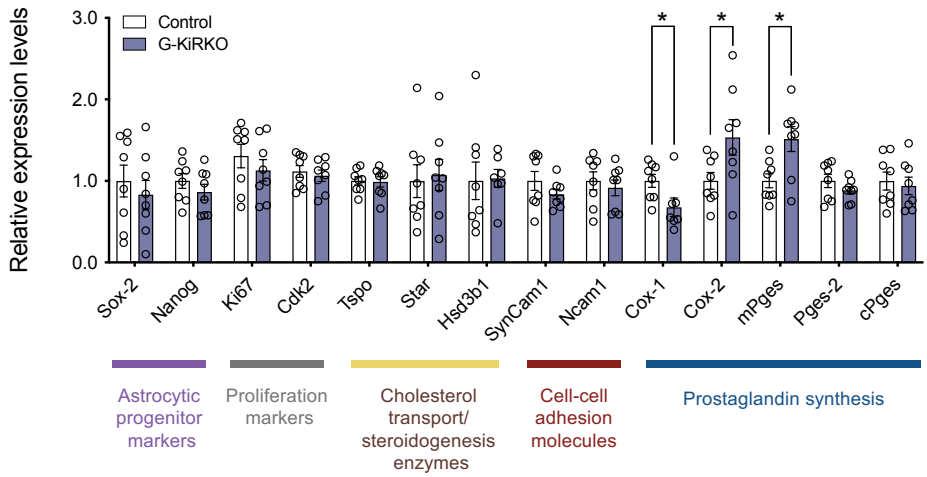
Relative expression levels
3.0
2.0
1.0
0.0
Control
G-KiRKO
*
*
*
Sox-2
Nanog
Ki67
Cdk2
Tspo
Star
Hsd3b1
SynCam1
Ncam1
Cox-1
Cox-2
mPges
Pges-2
cPges
Astrocytic progenitor markers
Proliferation markers
Cholesterol transport/ steroidogenesis enzymes
Cell-cell adhesion molecules
Prostaglandin synthesis

Figure 6